University of Stavanger

Faculty of Science and Technology

MASTER'S THESIS

Study program/Specialization: **MSc of Petroleum Engineering/ Natural Gas Engineering**	**Spring semester, 2016** **Open access**
Writer: **Pahmi Utamaraja Ginting**	…… (Writer's signature)
Faculty supervisor: **Jann Rune Ursin**	
Thesis title: **Effect of Colloidal Transport on CO_2 Injectivity**	
Credits (ECTS): **30**	
Key words: - **CCS** - **CO_2** - **Injectivity** - **Fines migration** - **Colloidal particle** - **Sandstone** - **Filtration**	**Pages: 61** **+ enclosure: 1** **Stavanger, 15th June 2016**

This page is intentionally blank

Dedication

This thesis is dedicated to my parents who always support and encourage me to obtain better education than themselves.

The thesis is also dedicated to my wife, Nindy Jayatri, for her support and love. Without her, this work would not have been accomplished.

Acknowledgement

I would want to thank the Norwegian State government for awarding me Quote Scheme scholarship to study in University of Stavanger.

I would also want to thank my supervisor, Prof. Jann Rune Ursin, for his help, motivation, guidance, advice, and encouragement through this thesis. Introduction story in every meeting always helps me to regain motivation.

Special thanks to PhD candidate, Yen Adams Sokama-Neuyam, for his help and guidance from beginning to the final phase of the experiment process and writing of the thesis. Thanks for sharing your experimental and analytical skills.

Finally, thanks to my friend, Bikram, for his constant help through the experiments.

Abstract

Climate change is a long term change in weather due to Earth process, volcanic activity and change concentration of greenhouse gases such as carbon dioxide (CO_2) in the atmosphere. CO_2 is generated mainly from industrial or human activity. Carbon Capture & Storage (CCS) is an alternative technique to capture anthropogenic CO_2, transport it to a suitable storage area, and finally store it safely and permanently in underground storage facilities. CO_2 could also be stored by another storage method such as geological storage, ocean storage, and mineral storage.

The primary option to store captured CO_2 is by injecting it into the geological storage in deep underground formation. Geological formation has great storage capacity to store huge amount of CO_2 and seal it permanently. A good storage capacity in geological formation need to go along with high injectivity to store large amount of CO_2. Also CO_2 could be injected with much lower energy in high injectivity formation, saving energy as a result.

CO_2 injection has several challenges. CO_2 injectivity is never always constant in the operation. A decrease in CO_2 injectivity waste energy and lower the efficiency. This injectivity loss is mainly caused by mineral precipitation, fines migration, and formation dry-out. Mineral precipitation and formation dry-out are mostly related to mineral or salt deposition inside formation, but fines migration is associated mineral dissolution.

Formation damage in subsurface porous media has been linked to fines migration. This formation damage induced by migratory fines takes place when fine particle travel together with reservoir fluid into the formation to reduce the flow channels and impair formation permeability and productivity. Therefore, fines migration could impair CO_2 well injectivity. CO_2 Injectivity loss could reduce the efficiency of CCS projects where large volumes of CO_2 is injected into the reservoir for storage.
In this research, we investigated the impact of fines migration on CO_2 injectivity. The influence of formation permeability, CO_2 injection rate and fines concentration on injectivity loss are the main parameter in this work.

The fines migration process was reconstructed by saturating the formation rock with external colloidal particles followed by CO_2 injection. Injection of stabilised colloidal particles into the

reservoir rock has almost the same behaviour as fines migration process. Pressure drop profiles were monitored throughout the experiments to quantify the effect of these colloids on CO_2 injectivity. Varying particle concentrations changes the pressure drop profiles. Low particle concentration tend to have flat pressure drop profile in saturated condition, high concentration tend to have increasing pressure profile showing there is more particle trapped inside the pore. This observation is also seen when particle size is increased. In some cases, filter cake has been observed. Permeability of the core is related to the size of the pore network. Low permeability core is characterized by narrow pore channels. The experiment shows that, in low permeability cores, pressure drop measured across the core is higher than in high permeability rock because of higher rate of entrapment of particle and filter cake formation.

CO_2 injectivity measurement shows that higher concentration of particles in the saturating brine induces higher injectivity loss as more particles are trapped within the pore channels of the core. It was observed that large particle sizes induced lower injectivity loss because filter cake formed near the inlet and restrained more particle from entering the core, resulting in less permeability decline. This was also observed in low permeability cores where the pore channels favour filter cake formation. Low injectivity loss was recorded as a result. Effect of CO_2 injection rate on colloidal transport and injectivity impairment was also investigated. The experimental results show that when CO_2 injection rate increases, the injectivity loss also increases.

This thesis will provide basic understanding of the mechanisms of fines migration in reservoir and how it could affect CO_2 injection and CCS operation as a whole.

Table of Content

List of Tables

List of Figures

Nomenclature

CCS	Carbon Capture Storage
CIF	Cumulative injected fluid
Cp	Colloidal particle concentration
Csp	Brine Concentration
d	Core diameter
EOR	Enhanced oil recovery
FW	Formation water
L	Core length
$m_{\text{dry core}}$	Dry core mass
$m_{\text{saturated core}}$	Brine saturated core mass
PV	Pore Volume
ΔP	Pressure drop
$\Delta P_{initial}$	Initial pressure drop
ΔP_{final}	Final pressure drop
q	Fluid rate of injection
Q	Gas injection rate
Q_{final}	Gas injection rate after particle injected
$Q_{initial}$	Gas injection rate before particle injected
t	Time recorded
Vb	Bulk volume
Vc	Colloidal particle volume
Vs	Solution volume
α	Injectivity index
ρ_b	Brine density
ρ_c	Colloidal particle density
ϕ	Porosity

1 Introduction

Statistics have shown that anthropogenic carbon dioxide (CO_2) emission has increased tremendously since the beginning of industrial era. Global warming and climate change have strong links to atmospheric greenhouse gases. These greenhouse gases are mainly by-products of fossil fuel combustion, electrical power generation, and, manufacture. Therefore, climate change is imminent unless steps are taken to reduce global carbon emission.

Carbon Capture & Storage (CCS) project is an alternative technique to reduce CO_2 emission in the atmosphere. CCS technology has the potential to reduce anthropogenic CO_2 emission from electric power generation and fossil fuel combustion by capturing the CO_2 and storing it in underground geological formations. CCS is implemented in three steps. First, industrial CO_2 is captured from sources such as electricity production, fuel processing, and industrial process. Second, the captured gas is transported to a designated area in pipelines or shipped in storage tanks. Finally, CO_2 is stored in safe and secure subsurface facilities such as ocean, deep saline formations, depleted oil and gas fields, and coal seam beds.

There are many ongoing and proposed geologic storage projects. Deep saline aquifer storage has been established at Sleipner field in Norway. About 1 Mt of CO_2 is stored per year. Injection of CO_2 at the Snohvit offshore facility on the seafloor of the Barents Sea started in April 2008 and is expected to have similar financial results as Sleipner. At full capacity, 700.000 tonnes of CO_2 will be stored each year (Karstad, 2002 and Statoil, 2010). Produced gas at Snohvit is transported by pipeline to Melkoya for processing. The shale formation in Snohvit field provides good seal for the storage to prevent CO_2 leakage.

Deep saline aquifers have the best storage capacity (IEA, 2016). This makes deep saline aquifers one of the most important underground storage facilities. However, storage capacity must be followed by high CO_2 injectivity for efficient operation. CO_2 injectivity loss is inevitable situation in CCS projects. Formation dry-out and salt precipitation have been found to strongly reduce CO2 injectivity in saline aquifers.

Mineral precipitation, formation dry-out, and fines migration are some of the major causes of CO_2 injectivity impairment. Sokama-Neuyam (2015) observed that brine salinity and mineral

deposition affect CO_2 injectivity. They found that mineral precipitation from formation water could reduce CO_2 injectivity. Mineral dissolution should improve formation permeability. The mineral around the pore network are dissolved which creates more open pore networks. However, dissolved minerals could gather together to become fines particle and migrate inside the formation. Fines migration transport particles into the pore network. The transported particles could be trapped within the pore channels plugging the core as a result. This situation could damage the formation by impairing permeability and porosity. The impaired permeability then increases CO_2 injectivity loss.

In this work, we investigated fines migration in core scale laboratory experiments. Sandstone core plugs was used to study fines migration and its impact on CO_2 injectivity. Fines migration is basically the transportation of fine particles in reservoir fluids. This process could be approached by injecting colloidal particles into the porous media. The permeability of the rock is used as the parameter to study the effect on CO_2 injectivity. Other parameters investigated in this work include the effect of CO_2 injection rate and particle size and concentration.

2 Problem Definition and Objectives

CCS is a promising technique to tackle climate change where atmospheric CO_2 is captured and stored in underground storage facilities. Therefore, adequate CO_2 injectivity is a prerequisite for such operations.

Fines migration is identified as a threat to formation permeability and CO2 injectivity. Fines migration proceeds from mineral dissolution that detach particles from the pore of rock. The detached particles are transported together with the formation fluid. Fines migration generally induces permeability decline. Mobilization of fines particle severely damage the formation performance (Khilar & Fogler, 1998). Most of the literature studied fines migration in water and oil. Also these studies did not highlight the effects of particle.

The objectives of this thesis are

- To investigate the effect of mineral dissolution and particle transport on CO_2 injectivity.
- To study the effect of key parameters such as particle size and concentration of fines, CO2 injection rate and initial rock permeability on CO_2 injectivity.

The goal is to obtain fundamental understanding of fines migration and its effect on CO_2 injectivity.

3 Theory

3.1 Carbon Capture and Storage (CCS): A Brief History and Future Prospects

Carbon dioxide (CO_2) is a chemical compound formed from two atoms of oxygen covalently bonded to one atom of carbon. It exits in atmosphere in a gas form at ambient temperature and pressure. Lacis A. (2010) pointed that CO_2 fraction in the breathable atmosphere is about 390 ppm.

Lucci *et al* (2011) explained that CO_2 is mainly produced from five process:

1. Combustion product of fossil fuels (oil, gas, coal) and wood.
2. Methane conversion to CO_2 as a by-product of hydrogen production plants.
3. Fermentation by-product in brewing process.
4. Thermal decomposition of limestone in the manufacture of lime.
5. As a by-product of sodium phosphate manufacture.

The emission of CO_2 has increased in the last two centuries due to industrialization and the increasing need for fossil fuels (Figure 1). This has led to one of the main causes of global warming.

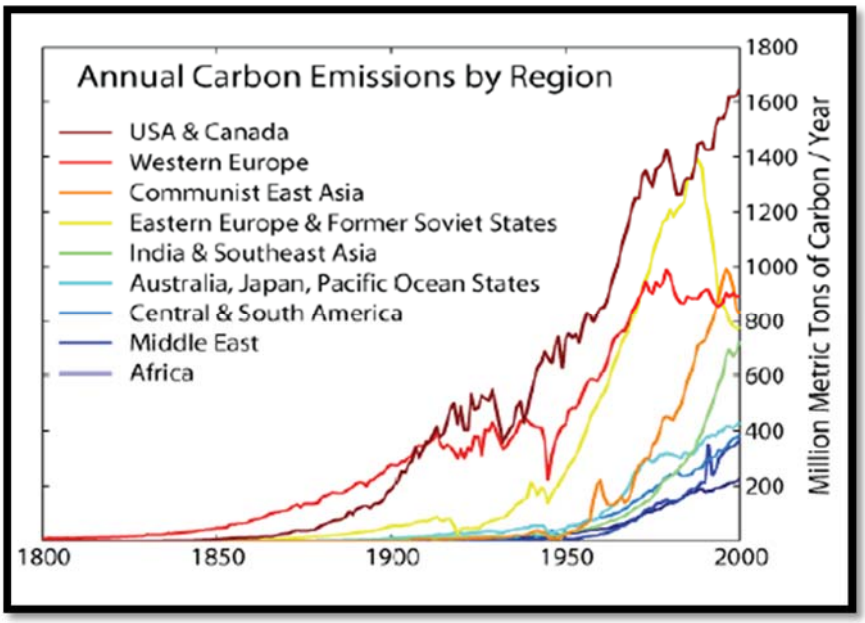

Figure 1. Global Carbon emission between 1800-2000. www.globalwarmingart.com

According to Hansen (2005), CO_2 is one of the main agents that increase solar radiation retention compared to other anthropogenic and natural causes. The consequences of this phenomenon are the increase of temperatures in the atmosphere, reduction of the volume of ices on earth's surface and the extinction of various animal species.

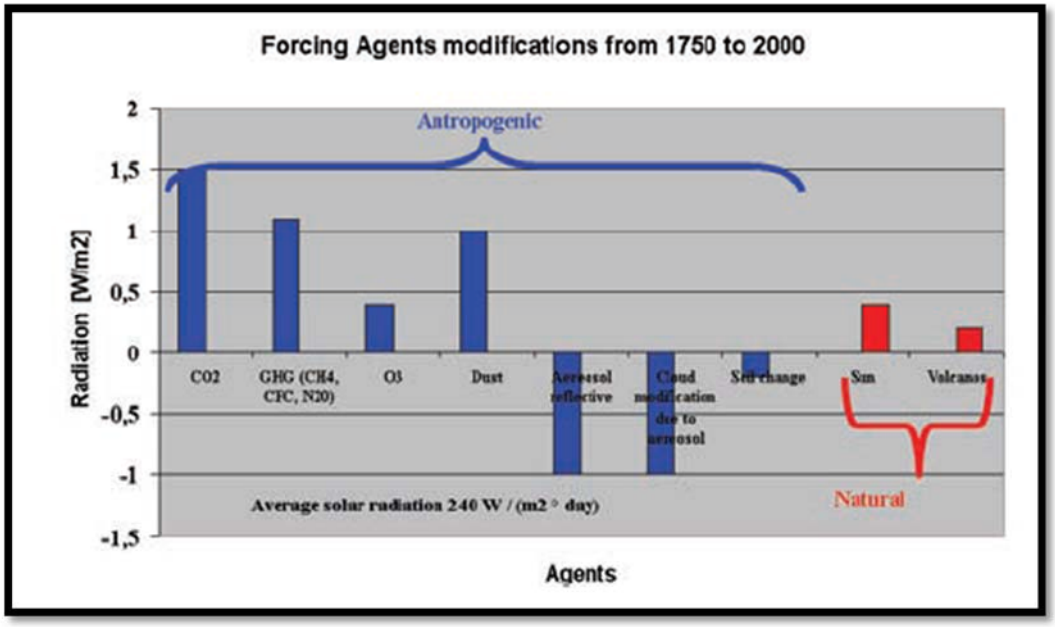

Figure 2. Hansen, 2005. Variation of climate "forcing agents" Between 1795-2000

According to the International Energy Agency (IEA) report, CO_2 in earth's atmosphere is considered a trace grade currently occurring at an average concentration of about 380 ppm by volume or 582 ppm by mass which the total mass of CO_2 is 3.10^5kg. Its concentration varies in different season and location. Concentration of CO_2 are generally higher in urban areas and specifically in indoor location it can reach ten times of background levels. Human activities which use fossil fuels and territorial expanding to forest have caused the concentration of CO_2 in atmosphere to increase by about 35% since the beginning of industrialization.

One mitigation option to reduce climate change is CO_2 capture and storage (CCS) technology. CCS is a process that consist the separation of CO_2 from industrial and energy-related sources, transport to a storage location and long-term isolation from the atmosphere. CCS has the potential to reduce overall mitigation costs and increase the flexibility in achieving greenhouse gas emission reductions.

There are three main separation or CO_2 capture systems: post-combustion, pre-combustion, and oxyfuel combustion. Post-combustion capture of CO_2 is economically feasible under specific

conditions. This type is used to capture CO_2 from part of the flue gases from a number of existing power plants. Pre-combustion capture involve the reaction of a fuel with oxygen or air and/or steam to produce a synthetic gas composed mainly of carbon monoxide and hydrogen (Tudori, 2010). Oxyfuel capture use nearly pure oxygen for combustion instead of air, resulting in a flue gas that is mainly CO_2 and water (Lucci, Demofonti, Tudori, & Spinelli, 2011).

Pipelines are preferred for transporting large amount of CO_2 for distances up to around 1000 km. in most gas pipelines, compressors at the upstream end drive the flow, but some pipelines need intermediate compressor stations. Shipping is preferred for larger distances overseas for volumes smaller than a few million tonnes of CO_2 where economically applicable. CO_2 can also be carried by rail and road tankers, but it is unlikely that these could be attractive options for large-scale CO_2 transportation.

Storage of CO_2 in deep, onshore and offshore geological formations uses many of the same technologies that is used by oil and gas companies. If CO_2 is injected into suitable saline formation or oil or gas fields, various physical and geochemical trapping mechanisms would prevent it from migrating to the surface. An essential physical trapping mechanism is the presence of caprock. The combination of CO_2 storage with Enhanced Oil Recovery (EOR) could lead to additional revenue from oil or gas recovery (IPCC, 2005). This is called Carbon Capture, Utilization and Storage (CCUS).

3.1.1 The Importance of CCS

As mentioned by Stangeland (2007), emission of greenhouse gases (GHG) will increase the average global temperature by 1.1 to 6.4 degree Celsius by the end of the 21st century (IPCC, 2005). A global warming of more than 2 degree Celsius increase in global average temperature will lead to serious consequences. Therefore, global GHG need to be reduced by 50-80 percent by 2050.

The consequences of high global warming could include melting of glaciers, leading to reduced water and food resources. Sea level will rise, and there will be more extreme weather, more draughts, and more floods. As a consequence, more than 200 million humans could become climate refugees. Ecosystems will be disrupted and 15-40 percent of all species could become extinct (Stangeland, 2007).

CCS is a key technology for tackling climate change in an affordable way, delivering economic and regional prosperity (Huhne Opens UK's first CCS plant, 2011). Industry already has the skills and experience to safely deliver CCS. CCS is one of a suite of technologies that will all be required to combat climate change, including renewables, nuclear and energy efficiency. IEA report (2010) highlighted the importance of CCS as one of the tools against global warming in which they reported that CCS could contribute to about 19% reduction in global CO_2 emissions by 2050 and that fighting climate change could cost over 70% more without CCS (Figure 3).

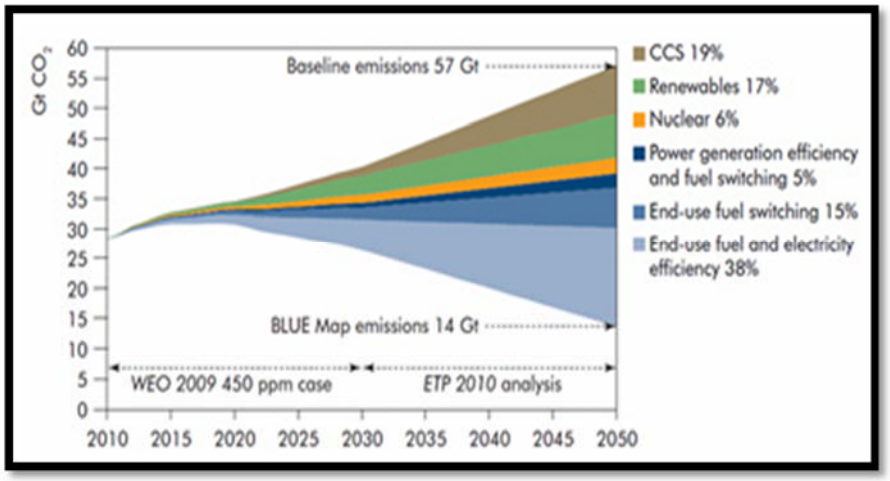

Figure 3. IEA Technology Perspectives 2010. OECD/IEA,2010

3.1.2 **Historical Review of CCS**

Since the 1950s, the oil and gas industry has spent billions of dollars developing CO_2 EOR technologies, commercial projects, and operations. The first patent for CO_2 EOR was granted in 1953. The Texas Railroad Commission (TRCC report) proposed CCS rule reported that the first three projects were in Osage Country, Oklahoma from 1958 to 1962. Another early CO_2 EOR project was in Jones County, near Abilene, Texas in the Mead Strawn field in 1964 (Holm). The first large-scale commercial CO_2 EOR project began operations in 1973 at the SACROC field in West Texas, which continues in operation today.

Most of the activity has been in land-based oil and gas fields due to the close proximity of fields with suitable geology to nearby economic sources of CO_2, however, research activities have been conducted for offshore oil fields for EOR as sources of CO_2 were available. Land based CO_2 EOR projects have steadily increased over the years based on the growing availability of

pipeline sourced CO_2 and expectations of oil prices sufficient to support the high upfront and operating costs of CO_2 EOR. Technology development have resulted in EOR performance improvements supporting additional investments in CO_2 projects.

CO_2 EOR projects had reached a global total of 127 (112 in USA) with 12 more planned for the USA, as reported in the EOR survey by the Oil and Gas Journal (O&GJ, 2010). Rising oil prices, low cost sources of high purity CO_2, and access to miscible fields with large amounts of unrecovered oil have supported growth in CO_2 based EOR which accounted for 272 mBbl/d (O&GJ, 2010)

In 1991, Norwegian government introduce tax on CO_2 emissions. It imposes a carbon tax equivalent to about $50 per ton of CO_2 released to atmosphere. Statoil has found Sleipner gas field in the North Sea, about 250 km west of Stavanger, Norway. The natural gas produces contains high concentration of CO_2 (about 9 %), while the market only requires 2.5%. In order to avoid the tax, in 1996, Statoil tested the technology by extracted the CO_2 and pumped it back deep underground to Utsira reservoir, deep saline aquifer, approximately 1000 m below the sea bed. The operation was considered successful. After 10 years of storage, 10 million of CO_2 has been stored and no sign of CO_2 leakage from the reservoir (Statoil, 2010).

CCS projects continue to develop in In Salah field, Algeria, in 2004 and Snohvit field, Norway in 2008. In Salah field has high CO_2 content about 5-10% in producing gas reservoir. CO_2 is reduced to 0.3% at the Krechba Central Processing Facility. The captured CO_2 is compressed and injected into waterleg of the Krechba Carbonifeorus reservoir through horizontal wells. Total CO_2 stored in In Salah field has reach 14-17 million tonnes. Snohvit field has CO_2 content about 5-8% in produced gas. Before the gas is transported to LNG plant in Melkoya, the CO_2 content has to be reduced to less than 50 ppm to prevent freeze-out during refrigeration process. Captured CO_2 is then stored to the reservoir. Total CO_2 stored in Snohvit field is 700000 tonnes per year. Both field are monitored with 4D seismic technology to detect movement of CO_2. And until now, no sign of leakage has been detected from reservoir (Statoil, 2010).

3.1.3 Sequestration Techniques

CO_2 must be kept and stored after it has been captured compressed and transported. The industry can either sequester the CO_2 or treat it as a commodity for commercial use. The value of CO_2 is dependent upon its level of contamination and the purpose intended (Kubus, 2010).

3.1.3.1 Geological Storage

Geological storage of CO_2 is accomplished by injecting it in dense form into a rock formation below the earth's formation. Porous rock formation which previously contained hydrocarbon fluid is potential candidate for CO_2 storage. There are three types of geological formation for CO_2 storage: depleted oil and gas reservoirs, deep saline formation, and unminable coal beds (IPCC, 2005). Figure 4 shows the options of geological storage.

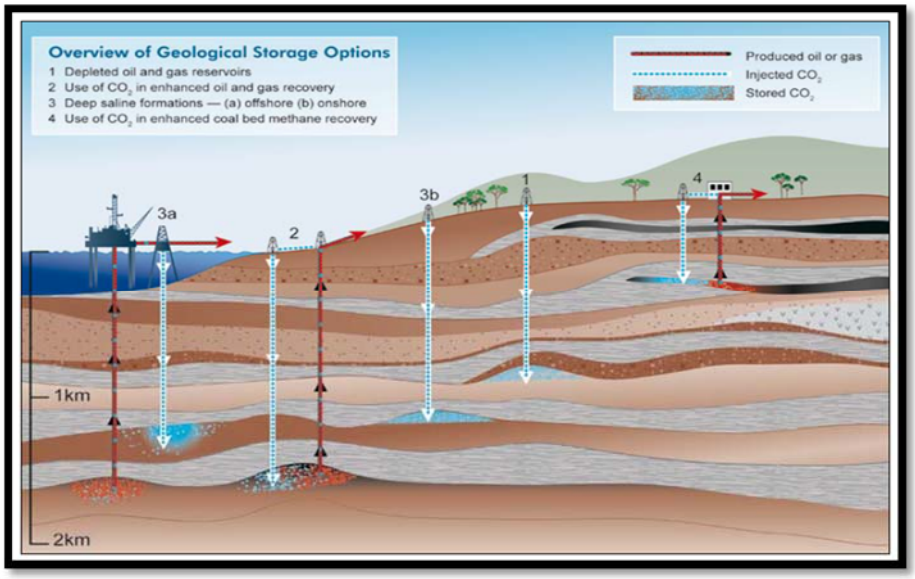

Figure 4. Method for storing CO2 in geological formation. The method can be combined with recovery method of hydrocarbon (EOR). (Courtesy CO2RC)

Depleted oil and gas fields

Depleted oil and gas fields have already proven their capability to hold oil and gas over millions of years and therefore have great potential to serve as long-term storage sites for carbon dioxide. Kubus (2010), cited that several fields had to be excluded from the potential storage sites due to geological, financial, safety, and technological reason. The characteristic of the potential reservoir for CO_2 storage are

- The reservoir capacity for storing CO_2 is more than 1 million tonnes CO_2.
- Only operated for CO_2 storage without any underground gas storage.

- The surface area of the reservoir is not highly populated.

In addition to CCS project, CO_2 is injected for EOR. Much of the CO_2 injected for EOR is produced with the oil, separated, and then reinjected. At the end of oil recovery, CO_2 is retained underground rather than vented to atmosphere.

Deep saline formation

Saline formations are deep sedimentary rocks saturated with formation waters or brines containing high concentration of dissolved salts. The saline formation or aquifer that is suitable for storage typically located at least 800 m depth and contain non potable water (Kubus, 2010). The appropriate area for storage should fulfil the following criteria:

- The reservoir should be deep enough to ensure CO_2 reach supercritical dense phase but still has good permeability and porosity.
- Have a good seal of caprock or impermeable layer.
- Sufficient capacity of CO_2 storage to be injected
- Effective petrophysical reservoir properties to ensure injectivity is economically viable and that sufficient CO_2 can be obtained.

Unminable coal beds

Coal contains fractures or cleats that impart some permeability to the system. Between cleats, solid coal has a very large number of microspores into which gas molecules from the cleats can diffuse and be tightly adsorbed. Coal can physically adsorb many gases and may contain up to 25 normal m^3 methane per tonne of coal at coal seam pressures (IPCC, 2005).

Larsen (2003) mentioned that the process of CO_2 trapping in coals for temperatures and pressures above the critical point is not well understood. The adsorption of CO_2 seems gradually replaced by absorption and the CO_2 diffuses or dissolves in coal. Carbon dioxide is a 'plasticizer' for coal, lowering the temperature required to cause the transition from a glassy, brittle structure to a rubbery, plastic structure (IPCC, 2005). In one case, the transition to temperature was interpreted to drop from about 400 C at 3 MPa to less than 30 C at 5.5 MPa CO_2 pressure (Larsen, 2003)

Kubus (2010) found the case in Hungary, the upper-Miocene lignite formations can be seen as potential CO_2 storage spots because these have large size area and are tectonically calm, but the

absorption quality is not very good, because the active storage absorption can take place only in mezzo and macro pores.

3.1.3.2 Ocean Storage

Oceans cover more than 70% of the earth's surface and the average depth is 3800 m. CO_2 is soluble in water, there are equilibrium process between atmosphere and water. If the CO_2 concentration in the atmosphere is higher than in the ocean, the ocean will gradually take up additional CO_2. This condition make the ocean a potential option for CO_2 storage (Figure 5).

CO_2 is directly injected into the deep ocean at depths at least 1000 m to ensure it is isolated from the atmosphere for centuries. CO_2 is transported by pipeline or ships to the ocean storage sites and then injected in to the water column at the sea floor. IPCC (2005) reported that the ocean storage has not yet been developed or demonstrated at a pilot scale.

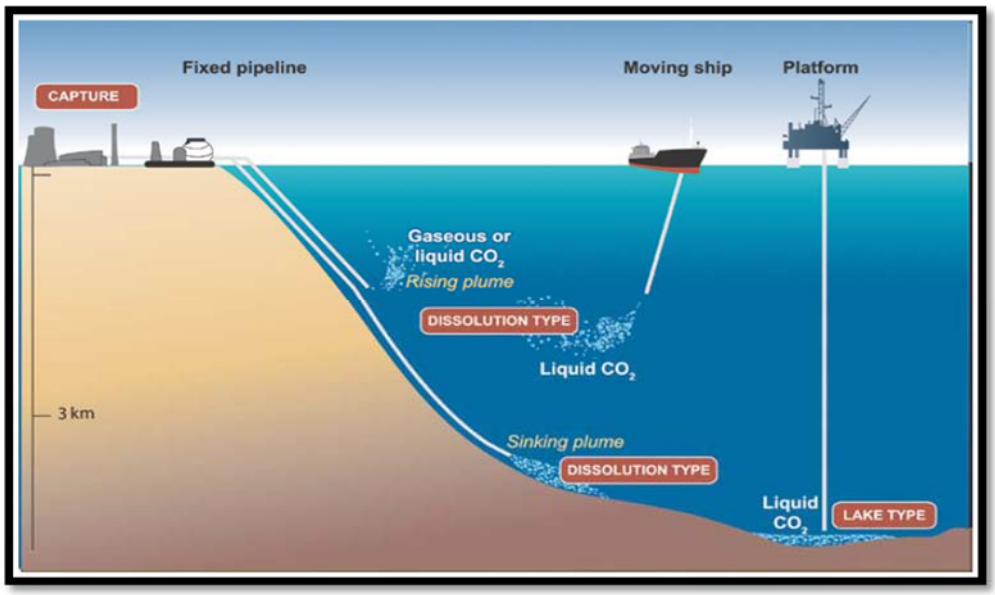

Figure 5. Overview of ocean storage concepts. Dissolution type ocean storage, the CO2 dissolves in the ocean water. Lake type ocean storage, the CO2 is initially a liquid on the sea floor (Courtesy CO2RC)

3.1.3.3 Mineral Storage

Mineral storage or mineral carbonation is based on the reaction of the CO_2 with metal oxide bearing materials to form insoluble carbonates with calcium and magnesium being the most attractive metals. Chemical reactions between these materials and CO_2 produces compounds such as magnesium carbonate ($MgCO_3$) and calcium carbonate ($CaCO_3$) (Figure 6).

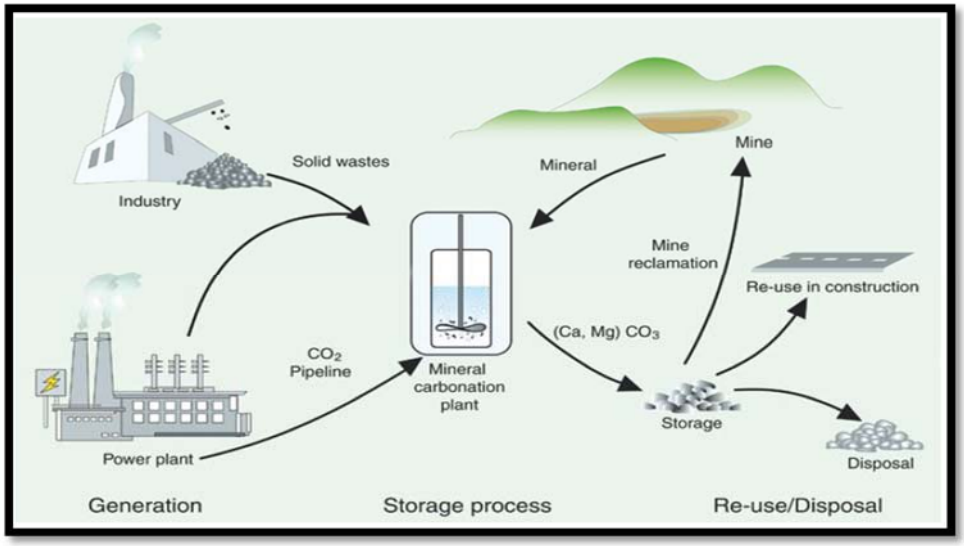

Figure 6. Process steps associated with the mineral carbonation of silicate rocks or industrial residues (Courtesy ECN)

The process of mineral carbonation occurs naturally, where it is known as 'weathering'. The process occurs very slowly so it need to be accelerated considerably to be a viable storage method for CO_2 captured from anthropogenic sources. Research in the field of mineral carbonation therefore focuses on finding process routes that can achieve reaction rates viable for industrial purposes and make the reaction more energy efficient (IPCC, 2005).

3.1.4 Industrial-Scale Projects in Norway

IPCC (2005), reported a number of pilot and commercial CO_2 storage projects which are under way or proposed. Most actual or planned commercial projects are associated with major gas production facilities that have gas streams containing CO_2 in the range of 10-15% by volume, such as Sleipner in North Sea, Snohvit in Barents Sea, In Salah in Algeria, and Gorgon in Australia.

Norway was one of the very first countries in the world that recognized and acted against global warming. Norway introduced the world's first CO_2 tax in 1991. In today's currency the tax amounted to about 60 US$/ton CO_2. This formed the backdrop against which the first CCS projects for climate change reasons came into operation in Norway (Kaarstad, 2008).

3.1.4.1 Sleipner

The Sleipner Project, operated by Statoil in the North Sea about 250 km off the coast of Norway, is the first commercial scale project dedicated to geological CO_2 storage in a saline formation. The CO_2 (about 9%) from Sleipner West Gas Field is separated, then injected into a large, deep, saline formation 800 m below the seabed of the North Sea. The Saline Aquifer CO_2 Storage (SACS) project was established to monitor and research the storage of CO_2. From 1995, the IEA Greenhouse Gas R&D Programme has worked with Statoil to arrange the monitoring and research activities. Approximately 1 $MtCO_2$ is removed from the produced natural gas and injected underground annually in the field. The CO_2 injection operation started in October 1996 and, by early 2005, more than 7 $MtCO_2$ had been injected at a rate of approximately 2700 ton/day. Over the lifetime of the project, a total of 20 $MtCO_2$ is expected to be stored (IPCC, 2005).

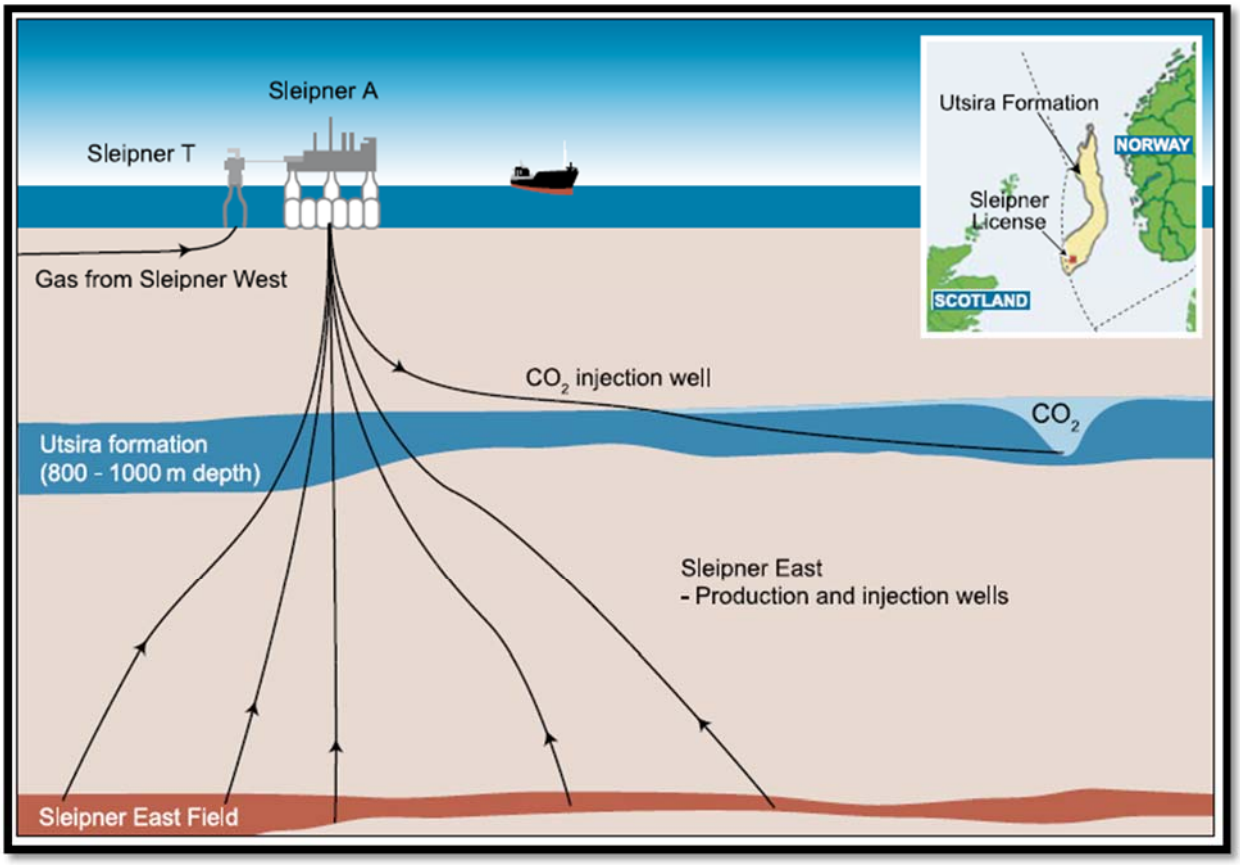

Figure 7. Diagram of the Sleipner CO2 Storage Project (IPCC, 2005)

IPCC, 2005 cited that the saline formation into which the CO_2 is injected is a brine-saturated unconsolidated sandstone about 800–1000 m below the sea floor. The saline formation has a very large storage capacity, on the order of 1–10 Gt CO_2. The top of the formation is fairly flat

on a regional scale, although it contains numerous small, low-amplitude closures. The overlying primary seal is an extensive, thick, shale layer.

The Sleipner CO_2 project commercially helped industry to reduce CO_2 tax. CO_2 emissions has been cut by almost million tonnes per year at an investment cost for the storage (not including capture) of about 100 million US$ in 1996. This project also verify that geological storage of CO_2 is a safe and reliable mitigation option (Kaarstad, 2008).

3.1.4.2 Snøhvit

Injection of CO_2 at the Snohvit offshore facility on the seafloor of the Barents Sea started in April 2008 and is expected to have good financial results like Sleipner. At full capacity, 700.000 tonnes of CO_2 will be stored each year (Kaarstad, 2008; Statoil, 2010). The natural gas with 5 to 8 % CO_2 is produced from the seafloor facility's subsea wells that tap a hydrocarbon reservoir overlying the CO_2 injection zone. A pipeline conveys the produced gas from the Snohvit field to Melkoya outside Hammerfest. A shale caprock lies above the sandstone and seals the CO_2 storage reservoir to ensure the CO_2 is confined underground without leaking to the surface (Sweatman, Crookshank, & Edman , 2011).

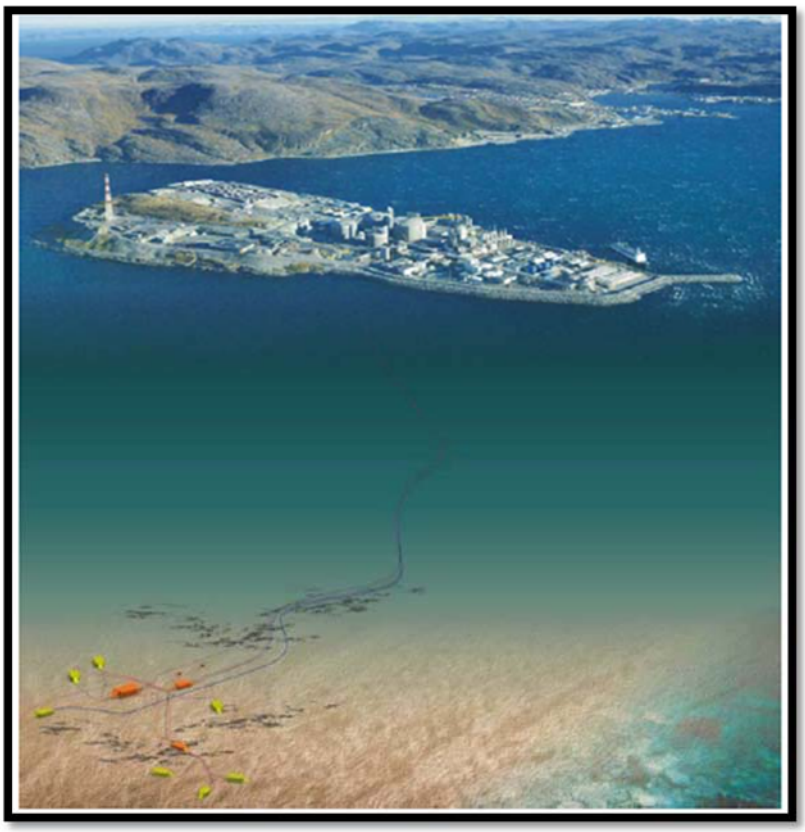

Figure 8. Snohvit seafloor facility pipelines, subsea wells and Melkoya LNG plants. (Sweatman, 2011))

As for Sleipner, the CO_2 tax provide an acceptable economic incentive to install a CO_2 compression facility including an 8 in CO_2 offshore pipeline with total length of 153 km and injection well into the Tubaen formation below natural gas reservoir. 0.7 million tons of CO_2 is injected annually based on the initial capital expenditure of about US$ 300 million (Kaarstad, 2008).

3.1.5 Future Prospects of CCS

High initial and uncertain capital cost of CCS operation give limited commercial application of CCS technology system. The cost for CCS can be split into cost of capture, transportation and storage. Current estimates for large-scale capture systems (including CO2 pressurization, excluding transportation and storage). If future efficiency gains are taken into account, costs could fall to economic level. With CO_2 transportation cost depends on distance. It is easy to minimize pipeline and shipment transportation cost. The storage site also give contribution to the cost. The location and injection method chosen can give differences in storage cost. Oil and gas filed for example can give revenue from using CO_2 for enhanced oil production (EOR).

Government must address CCS as an important project to advance technological understanding, increase efficiency and lower the cost. CCS should be considered as an alternative to sustainable energy system for the next 50 to 100 years (IEA, 2016). The important obstacle in the CCS operation is proving that CO_2 can be permanently and safely stored in underground to public. This is to get public acceptance to continue further the technology development and bring more additional benefit.

Report from IEA (2016) stated that the potential for 2030 is two to three orders of magnitude greater than the projected Mt-scale demonstration projects for 2015. This indicates the need to significantly increase both investment in RD&D and the scope of projects, if a CCS strategy is to succeed. A research and development program focus on storage projects must be prioritize. This has possibility to enhance production in oil and gas fields, brings more energy production in unminable coal bed, advance technology in ocean storage, and aquifer storage in low population density. Nevertheless, a regulatory and legal framework for CO_2 storage projects must be created to address issue around liability, licensing, leakage landowner, royalty, and citizens right (IEA, 2016).

3.2 Prerequisites for CCS

In CCS project, storage capacity is important to ensure CO_2 remains trapped for millions of years in subsurface. The criteria of storage capacity is an important point in the location decision. Furthermore, the injectivity performance of the reservoir play an important role in CO_2 storage operation.

3.2.1 Storage Capacity

Estimating the capacity for CO_2 geological storage can be done by differentiating the various mechanisms and means of trapping. In the oil and gas fields, the mechanisms of trapping is volumetric trapping. The capacity is the product of available volume of porous and permeable medium and CO_2 at in situ pressure and temperature. However, Oil and gas filed capacity estimations do not distinguish capacity relating to oil and gas that has already been produced from capacity relating to remaining reserves yet to be produced and that will become available in future years (IPCC, 2005). There is uncertainty about when oil and gas fields will be depleted and become available for CO_2 storage.

Saline formation has solubility trapping mechanism. The storage capacity is the amount of CO_2 that can be dissolved in the formation fluid. The location of formation can occur in sedimentary basin throughout the world. However, capacity estimation in saline formation can be a challenging process. The possible reason is multiple mechanism for storage including physical trap in low permeability caprock, dissolution and mineralization. The time frame for CO_2 storage also affect capacity estimates, the initial volumetric storage will change as CO_2 dissolves and reacts with minerals.

Adsorption is the trapping mechanism in unminable coal bed methane. The capacity is the product of coal volume and its capacity for adsorbing CO_2. As no commercial CO_2 in coal exists, the realistic assessment for storage in coal formation has not yet been made. But assuming CO_2 will be stored in coal formation without recovering CBM, Gale and Freund (2001) calculated the storage capacity of 3-15 $GtCO_2$ is achievable in coal formation worldwide.

3.2.2 Well Injectivity

Since large volume of CO_2 is injected into the formation, injectivity is an important aspect both in technical and economic issue for geological storage project. Injectivity is the capability of fluid to be injected into a geological formation. It is defined as the injection rate divided by the pressure difference between the injection point inside the well and formation. CO_2 injectivity should be significantly greater than brine injectivity, but Grigg (2005) found that the performance of CO_2 is not always the case. The injectivity was lower than expected and decreased over time. Injectivity changes is related to insufficiently known relative permeability effects (IPCC, 2005).

3.3 Well Injectivity Challenges in CCS

In CCS project, well injectivity play important role in efficiency of the project. As CO_2 is injected into the reservoir, rock characteristic, fluid characteristic, and CO_2 itself give significant effect to injectivity change. Mostly all these factors induce injectivity loss.

3.3.1 Formation Dry-out and Salt Precipitation

Reservoir fluid or formation water contain several ion and mineral in solution. Injection of CO_2 into the formation vaporises the formation water and causes salt precipitation. CO_2 displaces movable formation water and leaves residual formation water. The remaining formation water become more saline as CO_2 continues vaporizing it. As the concentration of formation water exceeds the critical supersaturation value (Zuluaga & Monsalve, 2003), salt will precipitate out of the solution. The precipitated salt fill the porous space and clog the pore network of the formation. This condition leads to permeability impairment and causes injectivity loss.

3.3.2 Mineral Dissolution and Fines Migration

Injection of CO_2 can impose different effect on the rock and fluid characteristic in the reservoir. The presence of clay mineral implies that injected fluids could interact with loosely attached clay fines to induce mineral dissolution and physical clay detachment. Pudlo (2014) observed there is permeability and porosity enhancement because of calcite and anhydrite dissolution. Due to dissolution, the open pore space is exposed to migrating fluids. He also found that the clay minerals detached from the grains. The fines particle comes into the fluid and migrates

inside the pore network. However, migratory fines could plug the pore throats and impair the petrophysical properties of the rock. This process can lead to permeability impairment as pore network can be plugged and blocked.

3.3.3 CO_2 Phase Changes

At normal temperature and pressure, carbon dioxide is a gas. The physical state of CO_2 varies with temperature and pressure. At low temperatures CO_2 is a solid; on warming the solid will sublime directly into the vapour state. At intermediate temperatures CO_2 may be turned from a vapour into a liquid by compressing it to certain pressure. In the gas phase, density of the CO_2 is low. This low density column of CO_2 can decrease the hydrostatic of the column and therefore decrease the bottomhole pressure. In the injection process, the pressure of CO_2 increases, resulting to the phase change. As quoted from Nimtz et al. (2010), a phase change from gas to liquid may result in instability in the flowrate and create cavitation in the flow pipe (Ramamurthi & Sunil Kumar, 2003).

3.4 Rock and Fluid Characteristics

3.4.1 Sandstone Rocks

Sandstone is a clastic sedimentary rock. It is composed of mineral grains with size between 1/16 mm and 2 mm diameter cemented together. Sandstone is deposited by water or air and can represent a number of different geologic environments. In many cases, the sand was deposited in shallow lakes or oceans, and beach environments. In others, the sands were deposited by large rivers and represent an inland river environment. Many are deposited in deltas where rivers empty into oceans. Some sandstones were deposited in ancient desert environments by blowing winds.

Sedimentology

From Alden (2013), sandstone is a sediment type of rock or a sedimentary rock. The sediment particles consist of clast of minerals and fragments of rock. Sandstone also has different kind of materials besides sedimentary particles. There matrix components are cemented together by cementing materials to become sandstone. Matrix is the very fine-grained material which is present within interstitial pore space between the framework grains. Cement is a mineral which

is either made from silica (chemically the same as quartz), calcium carbonate or iron oxide. Cement bind framework grain or fill the empty spaces between sediments.

Mineralogy

In addition to the framework grains, sandstones usually also contain other minerals which usually grow on the surface of the grains, or sometimes filling the pore space. The major mineral present in all sandstones is quartz (SiO_2) and followed by feldspar minerals such as illite and albite. Other identified minerals include glauconite, kaolonite, crysobalite and orthoclase which are minor in the composition (Mubiayi, 2013).

Clay Mineral

Most sandstone reservoirs contain clay minerals in some amount. The clay mineral type, abundance, and distribution generally affect the reservoir quality in terms of porosity, permeability, density, natural radioactivity, electrical conductivity, the water content of petroleum fields and reactivity to various enhanced oil recovery practises. The size of clay minerals are mostly less than four microns. The small size of clay minerals gives them high surface area which speeds up reaction with fluid.

Clay minerals are diverse groups of minerals which are members of the hydrous aluminous phyllosilicates (Deer, 1992). There are five dominant groups of clay minerals in sandstone (Worden & Morad, 2003):

1. *Kaolin-serpentine series clay minerals.* The chemical formula of kaolin in $Al_2Si_2O_5(OH)_4$, whereas the Mg end member serpentine has the formula $Mg_3Si_2O_5(OH)_4$. Kaolinite is the low temperature form which dickite and nacrite are thought to be the high temperature forms of kaolin.
2. *Illite and glauconite*. The general chemical formula for illite is $K_yAl_4(Si_{8-y},Al_y)O_{20}(OH)_4$, where *y* is typically significantly less than 2 (Velde,1985). Illite occurs as polytypes that reflect different ways in which layers are stacked. Galuconite has the formula $(K,Na)(Fe,Al,Mg)_2(Si,Al)_4O_{10}(OH)_2).nH_2O$. The facies terms typically includes Fe-rich marine clay minerals that range in composition to glauconitic mica.
3. *Smectite*. The general formula for smectite is $(0.5Ca,Na)_{0.7}(AL,Mg,Fe)_4(Si,Al)_8O_{20}(OH)_4.nH_2O$. Smectite has interlayer cations

which are hydrated resulting in the swelling characteristic of smectic clay minerals. Smectites are defined by their tendency to swell when exposed to organic solvents.

4. *Chlorite*. The general formula for chlorite is $(Mg,Al,Fe)_{12}[(Si,Al)_8O_{20}][OH]_{16}$. Chlorite occurs in a variety of morphologies.
5. *Mixed-layer clay minerals*. Mixed-layer clay minerals result from the interstratification of different mineral layers in a single structure (Srodon, 1999). Most mixed-layer clay minerals contain smectite as a swelling component, and include illite-smectite and chlorite-smectite (Worden & Morad, 2003)

3.4.2 Formation Brine

Formation brine is commonly found underground in reservoir or aquifer. Formation brine is formed during deposition of sedimentary rocks. The processes involved includes evaporation, retention of dissolved materials through membrane, deposition of solid, solution of other minerals, exchange of cations, bacterial and organic process, and other chemical process .The composition of formation brine has been shown to have effect on crude oil/brine/rock interaction, wettability, interfacial tension, relative permeability, and capillary pressure (Jadhunandan & Morrow, 1995; Basu & Sharma, 1997).

Synthetic brine solutions are used in many of the analytical procedure for analysing oilfield water (American Petroleum Institute, 1968). Such solutions are a necessity in the development of analytical methods to study the effects of possible interfering ions as close as formation brine. The representative compounds which is usually used to prepare synthetic brine are deionized water, NaCl, Na_2SO_4, $NaHCO_3$, KCl, $MgCl_2.6H_2O$, $CaCl_2.2H_2O$, and $SrCl_2.6H_2O$.

3.4.3 Characteristics and Behaviour of CO_2

Carbon dioxide (CO_2) is a chemical compound formed from carbon and oxygen, in the ratio of one to two. CO_2 gas has a slightly irritating odour, is colourless and is denser than air. It is existent in the atmosphere in small quantities (370 ppm) and gives contribution to Earth's environment as a necessary ingredient in the life cycle of plants and animals. In the photosynthesis process, plants assimilate CO_2 and release oxygen. Anthropogenic activities which cause the emission of CO_2 include the combustion of fossil fuels and other carbon-containing materials, the fermentation of organic compounds such as sugar and the breathing

of humans. Natural sources of CO_2, including volcanic activity, dominate the Earth's carbon cycle.

Physical properties of CO_2

At normal temperature and pressure, carbon dioxide is a gas. The physical state of CO_2 varies with temperature and pressure. At low temperatures CO_2 is a solid; on warming, if the pressure is below 5.1 bar, the solid will sublime directly into the vapour state. At intermediate temperatures (the temperature of the triple point, -56.5° C, and the critical point, 31.1° C), CO_2 may be turned from a vapour into a liquid by compressing it to the corresponding liquefaction pressure (and removing the heat produced).

At temperatures higher than 31.1° C (if the pressure is greater than 73.9 bar, the pressure at the critical point), CO_2 is in a supercritical state where it behaves as a gas but the density approaching or even exceeding the density of liquid water. This is an important aspect of CO_2's behaviour and is particularly relevant for its storage.

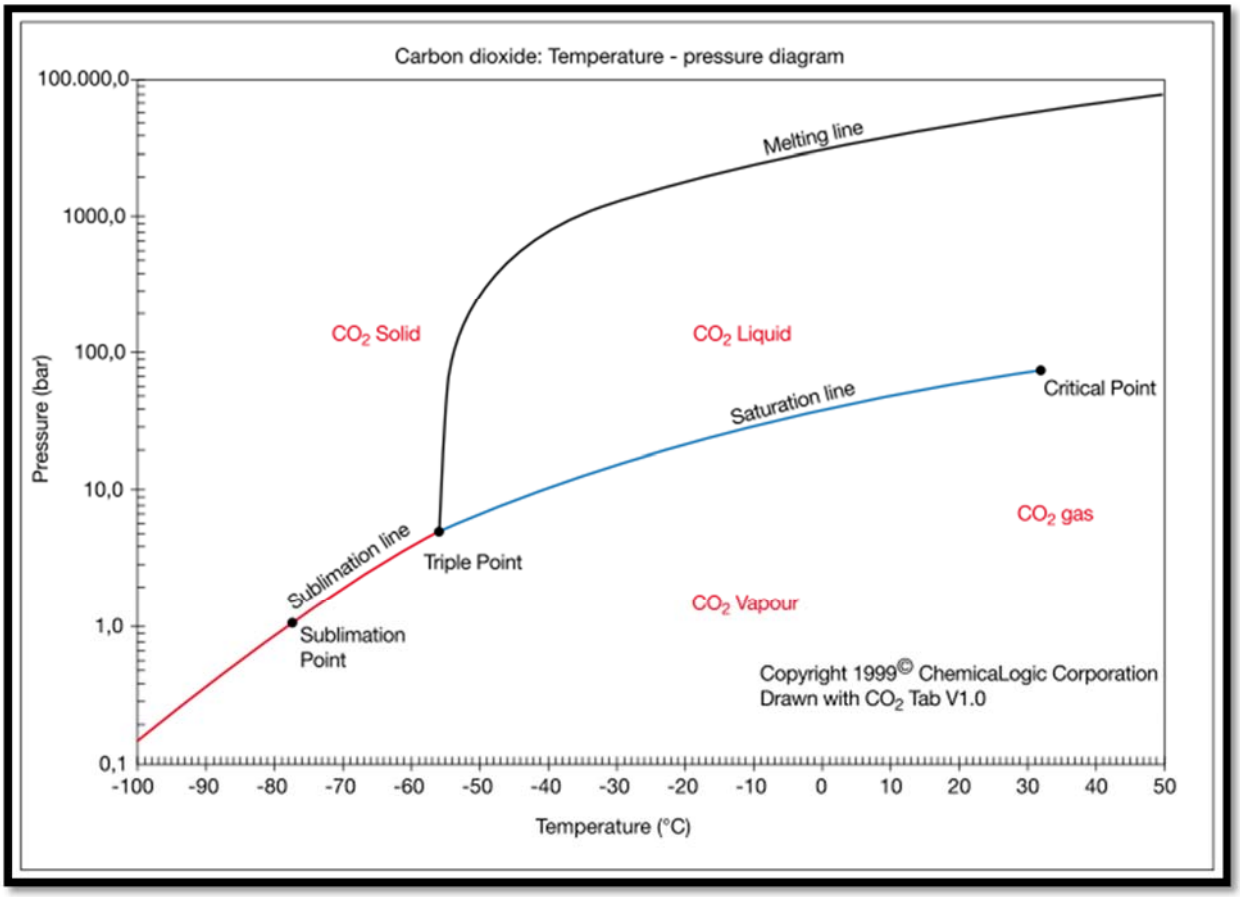

Figure 9. Phase diagram for CO_2. Copyright © 1999 ChemicaLogic Corporation

Heat is released or absorbed in each of the phase changes across the solid-gas, solid-liquid and liquid-gas boundaries. However, the phase changes from the supercritical condition to liquid or from supercritical to gas do not require or release heat. This property is useful for the design of CO_2 compression facilities since, if this can be exploited, it avoids the need to handle the heat associated with the liquid-gas phase change.

There is a substantial body of scientific information available on the physical properties of CO_2. Many authors have investigated the equation of state for CO_2 (Span & W., 1996). The variation of the density of CO_2 as a function of temperature and pressure and the variation of viscosity with temperature and pressure can be seen below.

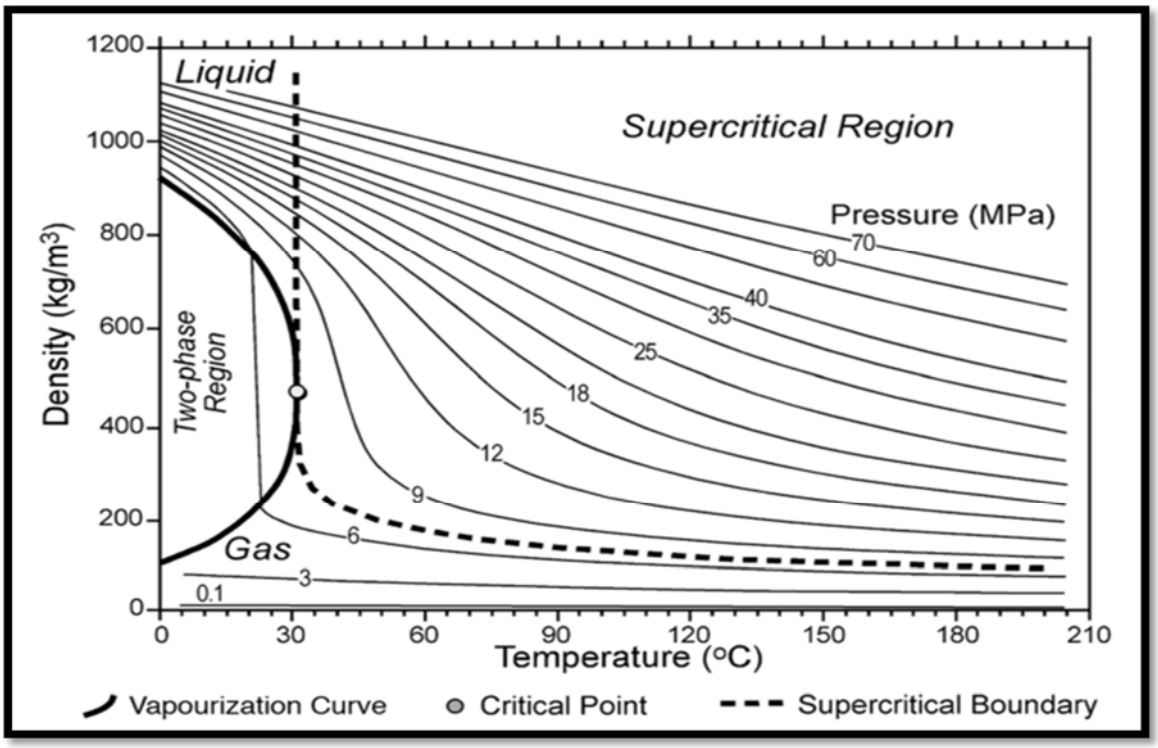

Figure 10. CO_2 density as a function of temperature and pressure (Bachu, 2003)

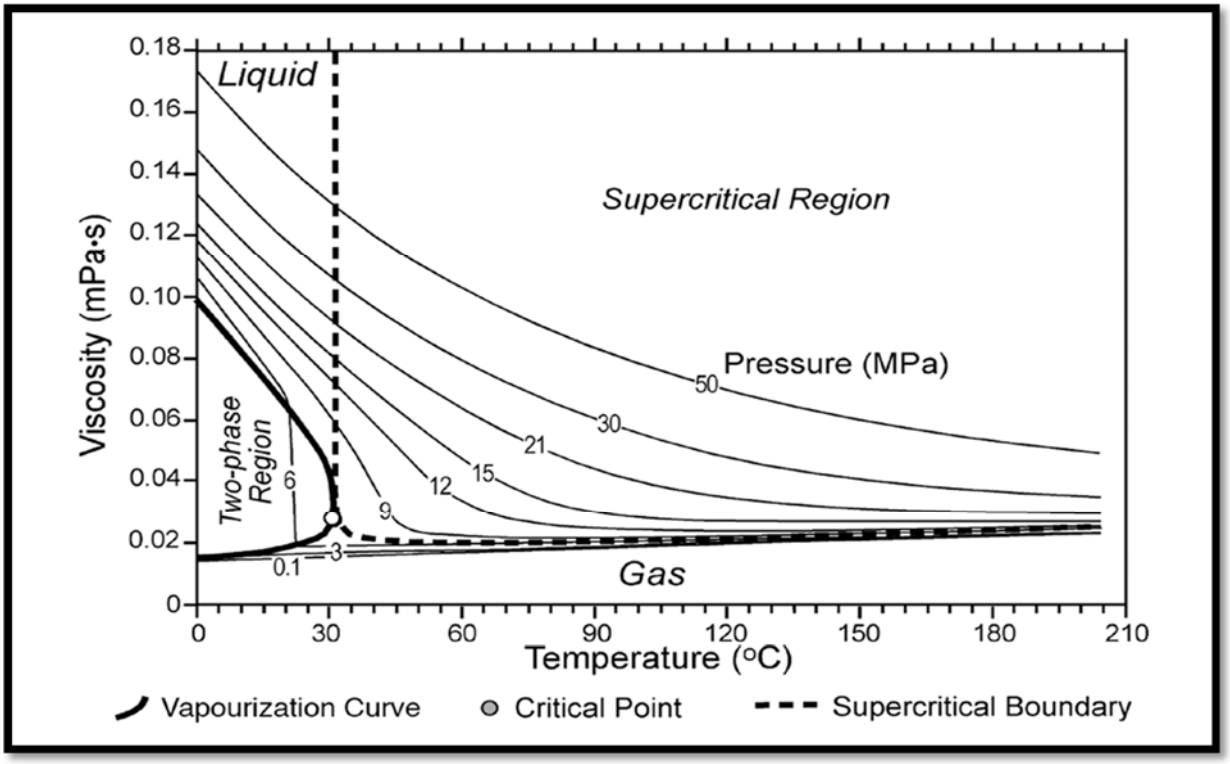

Figure 11. CO_2 viscosity as a function of temperature and pressure (Bachu, 2003)

Chemical properties of CO_2

In an aqueous solution CO_2 forms carbonic acid, which is too unstable to be easily isolated. The solubility of CO_2 in water decreases with increasing temperature and increasing pressure. The solubility of CO_2 in water also decreases with increasing water salinity by as much as one order of magnitude. The following empirical relation (Enick & S.M., 1990) can be used to estimate CO_2 solubility in brackish water and brine:

$$W_{CO2,b} = W_{CO2,w} \cdot (1.0 - 4.893414 \cdot 10^{-2} \cdot S + 0.1302838 \cdot 10^{-2} \cdot S^2 - 0.1871199 \cdot 10^{-4} \cdot S^3)$$

Where W_{CO2} is CO_2 solubility, S is water salinity (expressed as total dissolved solids in % by weight) and the subscripts w and b stand for pure water and brine, respectively. A solid hydrate separates from aqueous solutions of CO_2 that are chilled (below about 11°C) at elevated pressures. A hydrate is a crystalline compound consisting of the host (water) plus guest molecules. The host is formed from a tetrahedral hydrogen bonding network of water molecules; this network is sufficiently open to create pores that are large enough to contain a variety of other small molecules.

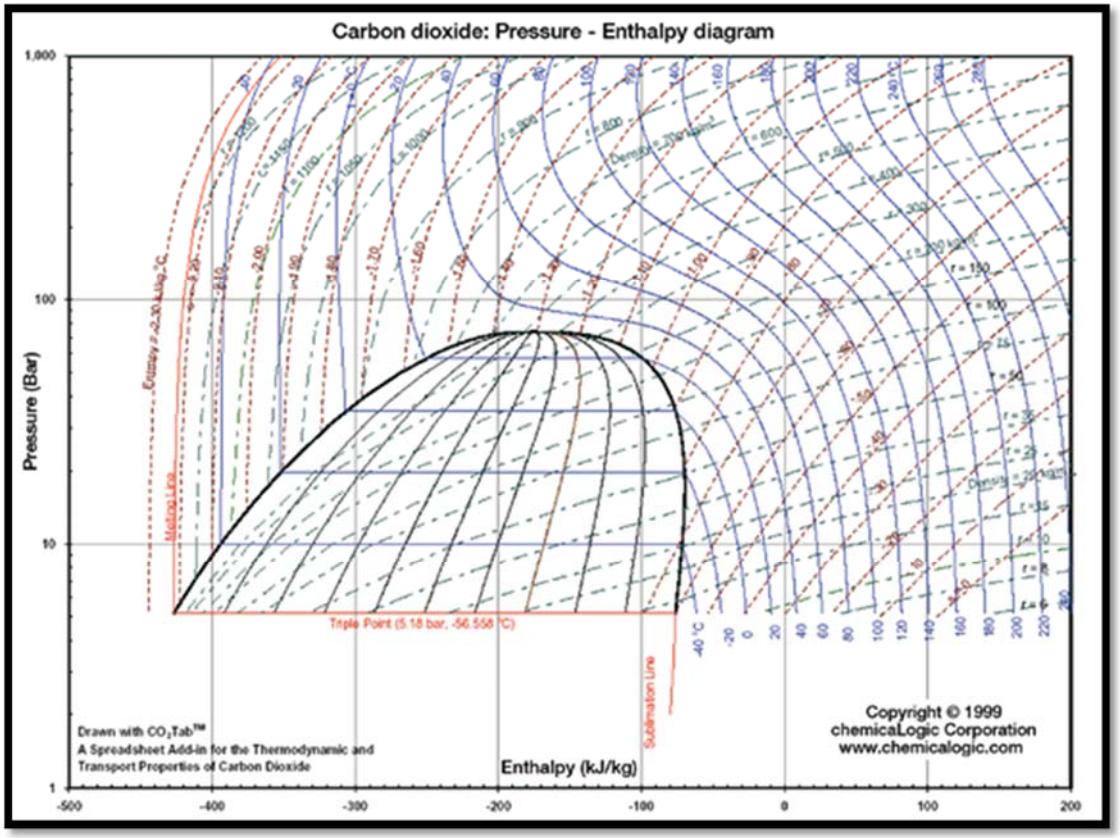

Figure 12. Pressure-Enthalphy chart for CO_2. Copyright © 1995-2003 ChemicaLogic Corporation

The dissolution of CO_2 in water (this may be sea water, or the saline water in geological formations) involves a number of chemical reactions between gaseous and dissolved carbon dioxide (CO_2), carbonic acid (H_2CO_3), bicarbonate ions (HCO^{3-}) and carbonate ions (CO_3^{2-}) which can be represented as follows:

$$CO_{2\,(g)} \leftrightarrows CO_{2\,(aq)}$$

$$CO_{2\,(aq)} + H_2O \leftrightarrows H_2CO_{3\,(aq)}$$

$$H_2CO_{3\,(aq)} \leftrightarrows H^+_{(aq)} + HCO_3^-{}_{(aq)}$$

$$HCO_3^-{}_{(aq)} \leftrightarrows H^+_{(aq)} + CO_3^{2-}{}_{(aq)}$$

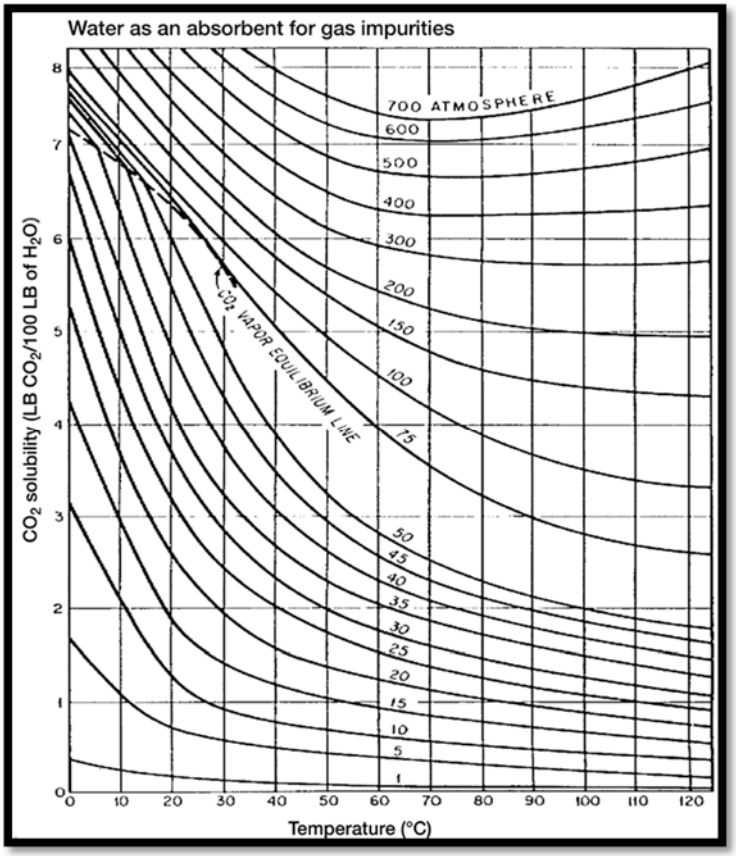

Figure 14. Solubiity of CO_2 in water (Kohl and Nielsen, 1997)

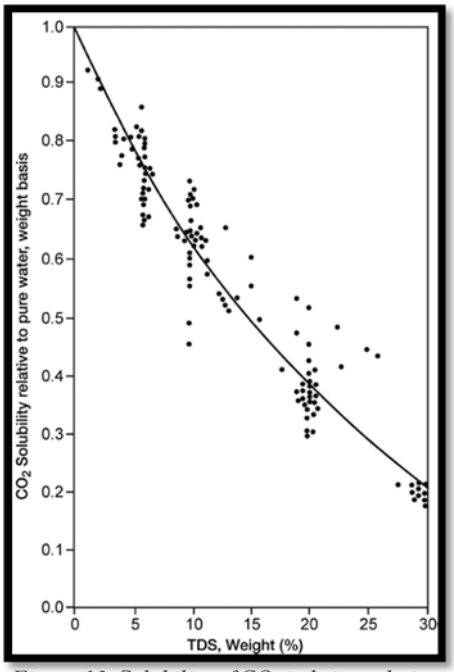

Figure 13. Solubility of CO_2 in brine relative to pure water.(Enick and Klara, 1990)

Addition of CO_2 to water initially leads to an increase in the amount of dissolved CO_2. The dissolved CO_2 reacts with water to form carbonic acid. Carbonic acid dissociates to form bicarbonate ions, which can further dissociate into carbonate ions. The net effect of dissolving anthropogenic CO_2 in water is the removal of carbonate ions and production of bicarbonate ions, with a lowering in pH.

3.5 Colloidal transport in porous media

3.5.1 Definition and Characteristics of Colloids

Colloid or colloidal solution is a heterogeneous mixture which has particle size from 1 -1000 nm. The particle and medium of colloid can be solid, liquid or bubbles. The colloidal particles are not seen by the naked eye, but they can be studied through ultra-microscope. Colloidal particle can pass through filter paper but are mostly captured in membrane filter. Colloidal particles move in random directions caused by the collision of the molecule. They move in constant motion. This movement is called Brownian movement. This movement distinguish between solution and colloids.

3.5.2 Factors Affecting Transport of Colloids in Porous Media

Transport of colloidal particle in porous media is associated with the particle capture and retention. The attachment of colloidal particles create a filtration effect inside the porous medium and consequently induce permeability decline. Particle filtration results in accumulation of particle in one location and leads to plugging or blocking of the pore network. Experiment from (Khilar & Fogler, 1998) shows that the particles filled up the porous medium and network resulting in less permeable and accumulation of particle inside the core.

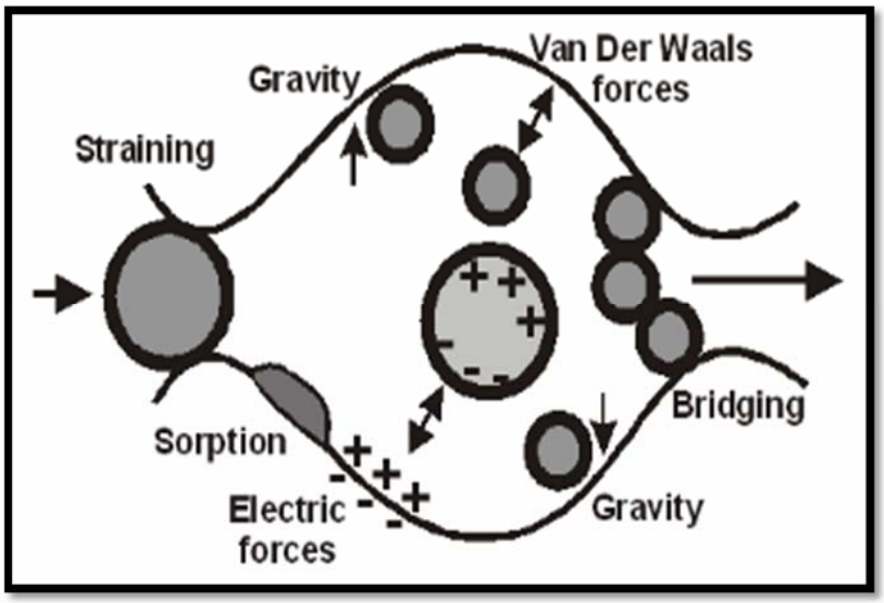

Figure 15. Multiple particle capture mechanism (Guedes, R.G, 2006)

3.5.3 Effects of Colloidal Transport on Well Injectivity

Well injectivity is directly related to the permeability of the formation. Colloidal transport causes formation damage. The movement of colloidal particles could fill the porous medium and plug the pore network, reducing the permeability of the formation.

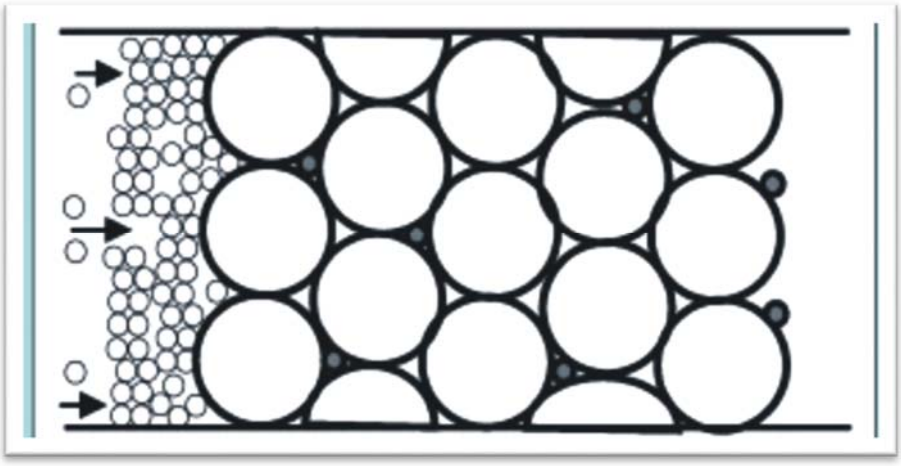

Figure 16. Fines migration and plugging situation (Fallah, AHmadi, Karae, & Rabani, 2012)

The permeability decrease means more pressure is required to inject fluid into the formation. More pressure required to inject the same amount of the fluid results in well injectivity change.

The size of particle and pore constriction or more pertinently, the size of fines particle to the pore constriction is the crucial parameter to determine the entrapment or piping mechanism would occur in the pore throat (Khilar & Fogler, 1998). If the size of fines is larger or the same as the size of pore throat, certainly plugging or blocking of the pore throat would occur.

Size of fines / Size of pore constrictions	Occurrence
≥1	Plugging due to blocking or size exclusion
0.1 to 0.6	Plugging due to bridging and multiparticle blocking
0.04 to 0.10	Plugging due to surface deposition, bridging, and multiparticle blocking
0.01 to 0.04	Surface deposition. Multiparticle blocking may or may not occur
less than 0.01	Piping

Table 1. Dependence of plugging or piping on the ratio of size of fines to size of pore constrictions (Khilar & Fogler, 1998)

3.5.4 The Role of Colloidal Transport in Well Injectivity and CCS

A colloidal transport has a role in many industrial applications. It ranges from particle filtration and fines migration in reservoir. Fines migration can lead to formation damage and permeability decline which causes injectivity change. The injectivity change can affect CCS operation significantly. To introduce CO_2 into the storage formation, high well injectivity is preferred to store large amount of CO_2. The injectivity loss caused by permeability impairment from particle capture in fines migration reduce the performance of the project.

4 Pre-Experimental Work

4.1 Mineral Dissolution in CCS: A Laboratory Approximation of the Problem

In this experiment we assume that mineral dissolution detach particles and lead to fines migration. This condition is approached by saturating the porous medium with colloids. Sandstone core is saturated by injecting colloidal solution of specific particle size and concentration. Colloidal transport within the sandstone core is monitored through pressure drop measurements across the core.

4.2 Laboratory Core-Flood Experiments

In CCS, CO2 is injected into subsurface porous media. The difference of pressure and temperature between the surface and the formation will give a phase change to CO_2. At formation condition, CO_2 is expected to be in supercritical phase. This condition is implemented in laboratory condition. The gas injected is given specific pressure and temperature at which the phase of CO_2 is in supercritical condition. CO_2 is injected from the inlet of the core with even pressure distribution. Confinement pressure is applied to the core to avoid fluid bypass from inlet to outlet.

4.3 Selection of Experimental Materials and Conditions

Three important materials were used in this experiment. They are sandstone core, colloidal particle, and CO_2. All the materials were carefully selected and conditioned to get as close as possible approximation practical field conditions. The properties and behaviour of the materials were tuned to match the experiment objectives.

Sandstone core is an indispensable material in this experiment. The reservoir was represented by sandstone core plugs. Sandstone core has the same pore size distribution as the real reservoir. Berea and Kirby sandstone core samples respectively represents high and low permeability formations. Different properties of the core were chosen in order to run sensitivities in the experiment.

Khilar& Fogler (1998) stated that colloidal particles in general carry a surface charge which depends on how the fines are formed. He also stated that surface charges are generally acquired through the adsorption of specific ions from the solution. In migration, this charge play a role in the process of release, migration, and capture of the particles. In this experiment, stable and neutral colloidal particles were selected to eliminate or at least minimize interactions between the particles and the porous media.

The temperature and pressure in the reservoir is expected to change the phase of CO_2 to supercritical phase. Supercritical CO_2 is achieved when the pressure is above 75 bar and temperature higher than 30 ^oC. The pump and oven are set to achieve these vital experimental conditions.

4.4 Key Parameters and Measurement Procedures

Only the physical aspects of fines migration and CO2 injectivity were studied. CO_2 is injected into the core at certain flowrate and pressure. Flowrate and Injection pressure is set and directly measured from the injection pump. Pressure drop is measured by the pressure transducer. Pressure sensor is installed exactly in the inlet and outlet of the core. Outlet pressure is also recorded to ensure the stability of the phase of CO_2.

Pressure difference and flow rate are mainly the key parameters of the experiment. Those two parameter will give the injectivity index which is defined by Buret et al. (2010),

$$\alpha = \frac{(\Delta P_{initial}/Q_{initial})_{CO2}}{\left(\Delta P_{final}/Q_{final}\right)_{CO2}}$$

As initial and final flowrate is equal, the above formula can be simplified to following equation

$$\alpha = \frac{(\Delta P_{initial})_{CO2}}{\left(\Delta P_{final}\right)_{CO2}}$$

From injectivity index above, the injectivity loss is simply defined as

$$Injectivity\ loss = (1 - \alpha) \times 100\%$$

Where $(\Delta P_{initial})_{CO2}$ is the pressure drop across the clean core and $\left(\Delta P_{final}\right)_{CO2}$ is pressure drop after the core is saturated.

4.5 Uncertainty and Error Analysis

4.5.1 Uncertainty

The experimental results were measured with equipment that has uncertainty. Human error also contributes to the uncertainty; handling equipment, measurement bias, and calculation assumption. Environmental conditions such as room temperature, ambient pressure, leaks, and equipment failure also add uncertainties.

4.5.1.1 Pressure and Temperature Variation

In order to reach the desired phase of CO_2, pressure and temperature need to be adjusted and kept constant. The injection line is coiled to ensure a long exposure to heat from the oven. The temperature of the oven is set higher than supercritical temperature to avoid phase change. The pressure is also maintained at slightly higher than supercritical phase. Any variation of the temperature and pressure can affect the property of the gas such as viscosity and density in the experiment. This can result in different pressure drop readings and different injectivity change.

4.5.1.2 Equipment Uncertainties

All equipment in this experiment came with uncertainty from the manufacturer. It is important to be aware that the measured values may vary between certain intervals. Each measurement has specific uncertainty value.

Equipment	Measurement	Uncertainty	Unit
Pressure transducer	Pressure	± 0.008	bar
Thermometer	Temperature	± 0.05	^oC
Digital balance	Mass	± 0.0005	g
Measurement glass	Volume	± 0.05	L
ISCO Pump	Pressure	± 0.05	bar
	Flow	± 0.05	ml/min
Quizix Pump	Pressure	± 0.05	bar
	Flow	± 0.0005	ml/min

Table 2. Equipment Uncertainties

4.5.1.3 Assumptions

Several assumptions were made in order to simplify the experimental work while at the same time maintaining key processes that are relevant to practical CO_2 injection. These are the assumptions made in the experiment.

- Colloidal particles is well dispersed and stable during saturation
- No fluid bypass during injection
- CO_2 phase changes are negligible
- The core is at the oven temperature
- Room temperature is constant at 20 ^oC
- No leakage during injection

4.5.2 Error Analysis

A measurement of physical quantity in the experiment is always an approximation. The deviation of measured value rises from different sources. The error in experiment needs to be stated to determine the validity of the experimental results. In general, there are three types of error which uncertainty in measurement arises.

1. Systematic errors

   These errors affect the accuracy of the measurement. These error comes from the imperfectly made instrument, improper calibrated, and poor experimental technique. Number of observation sample cannot reduce the systematic error. It can only be reduced by applying correction factor or improve experimental skill.

2. Random errors

   These error comes from unknown and indeterminate experimental situation. Instrument resolution and physical variation are the example of random error that could arise in the experiment. Random error can be decreased by obtaining and averaging large number of observation.

3. Personal Errors

   Carelessness, bias, and poor technique of the experimenter give personal errors to the experimental result. Incorrect measurements, poor technique, and a bias by expecting expected value brings error result. Random error can be avoided by improving the technique and repeating the measurements.

4.5.3 Accounting for Errors

In the experiment, the result has to be compared to other known or experimental values. The percentage difference of the value from several observation need to be found in order to get the acceptable result. In most cases 10 % of percent error or difference is acceptable. This is to indicate the accuracy and precision of the experimental measurement.

1. Percent error

   Percent error is used to compare the experiment result with the accepted value. It is the absolute value of difference of experimental value and known accepted value divided by accepted value. This error comes in this formula

$$\%\ error = \frac{|experimental\ value - accepted\ value|}{accepted\ value} \times 100\%$$

2. Percent difference

   Percent difference is used when there is no known accepted value. It is obtained by comparing one experimental result to another experimental result. It is the absolute value of difference of the values divided by average values. This error comes in this formula

$$\%\ difference = \frac{|experimental\ value\ 1 - experimental\ value\ 2|}{average\ values} \times 100\%$$

3. Mean and standard deviation

   In multiple measurements, the measured value will approach the central value (Carlson, 2000). The measured values are grouped into a distribution. The distribution is described by mean and standard deviation values. Mean is the central value. Mean is calculated from the set of N measured values for some quantity x. Mean is represented in symbol $< x >$.

$$\langle x \rangle = \frac{1}{N}\sum_{i=1}^{N} x_i = \frac{1}{N}\left(x_1 + x_2 + x_3 + \cdots + x_{N-i} + x_N \right)$$

   Standard deviation is the spread or deviation of measured value about the mean (Carlson, 2000). Standard deviation is represented by the symbol σ and calculated from this formula

$$\sigma_x = \sqrt{\frac{1}{N-1}\sum_{i=1}^{N}(x_i - \langle x \rangle)^2}$$

5 Experiments

5.1 Experimental Objectives

The purpose of the experiments is to investigate the physical effects of fines migration on CO_2 injectivity in sandstone reservoir rock. Parameters studied include the colloidal particle concentration, colloidal particle size, gas injection rate, and rock permeability. The experimental work is sectioned as follows:

1. Colloidal particle injection.
2. Supercritical CO_2 injection.
3. Liquid CO_2 measurement.

5.2 Experimental Materials

Various materials were used in this experiments. The components and the process used to prepare the fluid, particle, and rock materials is discussed in this section.

5.2.1 Fluid

Gas

The gas used is liquefied CO_2 with purity percentage of 99.7%. It is purchased from Yara Praxair AS, Oslo in the container of 30 kg cylinder.

Colloidal Particle

Latex particles made of fumed alumina oxide from Evonik Industries were used for the preparation of colloids. A milky white appearance dispersion with special anionic stabilization and neutral pH value. High pH solution (>7) and low salinity brine prevents colloids from aggregation and from attachment to the surface of the rock. The properties of particle are presented in the table below.

	Aerodisp W640 ZX		Aerodsip W 630	
Properties and test methods	Unit	Value	Unit	value
Al_2O_3 content	%	39-41	%	29-31
Viscosity	mPa/s	<70	mPa/s	<2000
pH		6.0-9.0		3.0-5.0
Density	g/cc	1.39	g/cc	1.26
Particle size	µm	0.08	µm	0.14

Table 3. Properties of colloidal particles (Evonik Industries)

Brine

Two types of brine were used in this experiment. Brine is used to prepare the colloidal solution. The component of the brine is only NaCl with concentration of 5 g/l. This brine is also used for diluting the colloidal solution. A different brine was prepared as synthetic formation water with salinity of about 105.51 g/l (Table 4). This brine was used to saturate the core before measuring the base injectivity loss of the core.

Salt	Concentration (g/l)
NaCl	77.4
Na_2SO_4	0.13
KCl	0.42
$MgCl_2.6H_2O$	3.56
$CaCl_2.2H_2O$	21.75
$SrCl_2.6H_20$	2.25

Table 4. Composition of synthetic formation water (Fjelde et al. 2013)

5.2.2 **Rock**

This experiment used two sandstone core sample purchased from Kocurek Industries, USA. Berea sandstone core sample has relatively high porosity and high permeability properties and Kirby sandstone sandstone core which has much lower permeability compared to Berea. The dimension of core sample is 20 cm long and 3.81 cm diameter. Characteristics and components of the core are presented in Table 5.

Core sample	Brine Perm (mD)	Gas Perm (mD)	Porosity (%)	Formation
Berea	60-100	200-315	19-20	Kipton
Kirby	9	30	21	Edwards Plateau

Table 5. Characteristic on sandstone core sample (Courtesy of Kocurek Industries)

Mineral	Formula	Percentage
Silica	SiO_2	93.13%
Alumina	Al_2O_3	3.86%
Ferric Oxide	Fe_2O_3	0.11%
Ferrous Oxide	FeO	0.54%
Magnesium Oxide	MgO	0.25%
Calcium Oxide	CaO	0.1%

Table 6. Mineral component of Berea sandstone core sample

5.3 Experimental Setup

Two experimental set-ups have been used to carry out the experiment. Existing experimental set-ups were available from previous CO_2 injectivity loss research conducted at University of Stavanger (Sokama-Neuyam, 2015). The first set-up is intended to saturate the core with brine or colloidal particle and inject supercritical CO_2 into the core. The second set-up is used only for measuring the liquid CO_2 permeability of the core.

In the first set-up (Figure 17), Quizix pump is used to deliver the brine or the colloidal particle into the core. CO_2 from the gas cylinder is sent to ISCO CO_2 pump with temperature being maintained by a cooler. Long core holder with dimension of 36 cm long is placed inside an oven at constant temperature. Long coiled tubing is put inside the oven and connected to the inlet of the core holder to ensure the fluid achieves thermal equilibrium. Differential pressure transducer is connected to both end of core holder to measure the pressure drop across the core sample. The hydraulic pump is connected onto the core holder to provide overburden pressure. Two backpressure regulators are connected at the outlet of core holder to control the injection pressure of brine and CO_2. Piston cell is connected to the backpressure gauge to collect CO_2. Measuring glass is connected to the backpressure gauge to collect brine or colloidal particle effluent.

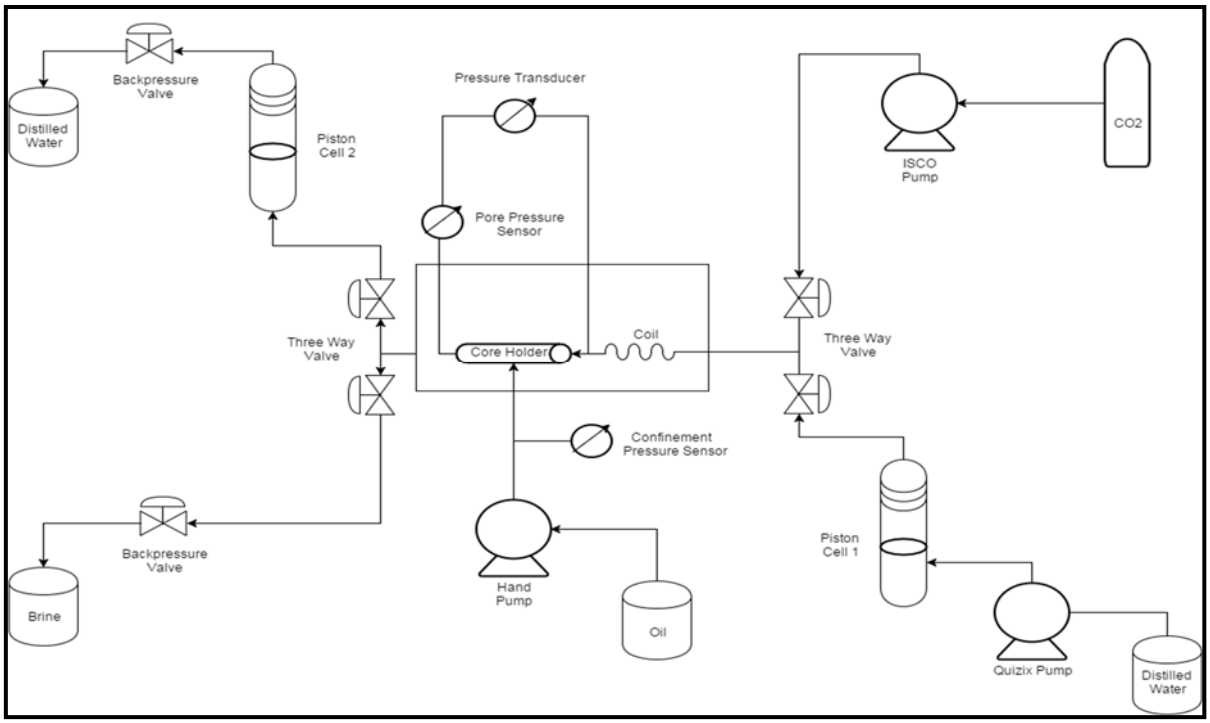

Figure 17. Experimental Set-up 1

Pressure-tapped coreholder is used to measure liquid CO_2 permeability in the second set-up (Figure 18). It is used to measure pressure drop in different sections of the core.

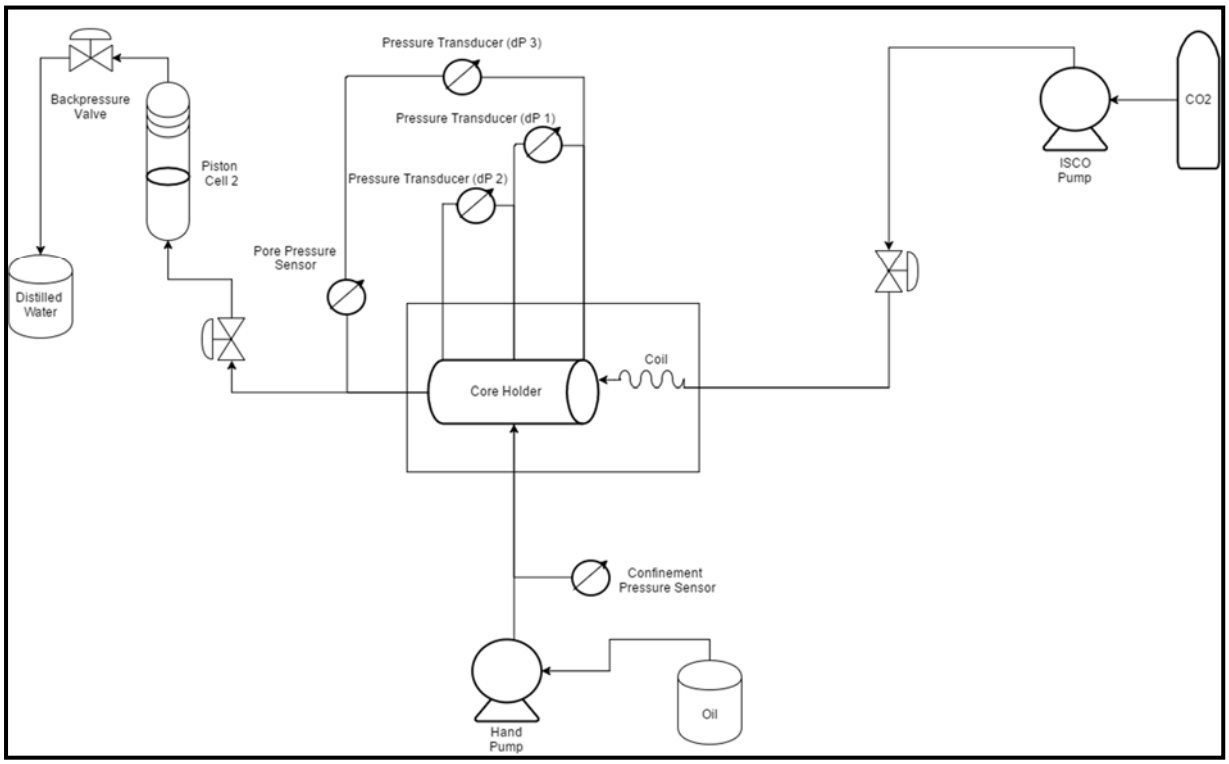

Figure 18. Experimental Set-up 2

5.4 Experimental Procedures

5.4.1 Preparation of Brine and Colloidal Particle

Brine is prepared from the mineral components and deionized water. The solution then is agitated with magnetic stirrer for at least 2 hours. After the stirring process, the synthetic brine is filtered with 0.22 μm filter paper to remove contaminants. The density of brine is then measured with density meter.

The colloidal solution is prepared by mixing the colloidal particles and low salinity brine. The colloids is stirred with magnetic stirrer for 24 hr to ensure stability of the colloids. The solution is then filtered with 0.22 μm filter paper. The required volume of colloidal particle to prepare a certain concentration is calculated as

$$V_c = \frac{V_s \times \rho_b \times C_{sp}/100}{\frac{C_p}{100} \times \rho_c}$$

Where V_c is the required volume of colloidal particle, V_s is the desired volume of solution, ρ_b is the density of the brine, C_{sp} is the desired concentration of the brine, C_p is the concentration of colloidal particle, and ρ_c is the density of colloidal particle.

5.4.2 Calculation of Pore Volume and Porosity

The bulk volume can is determined by direct calculation. From the dimension of the core, the bulk volume is calculated as

$$V_b = \frac{\pi d^2 L}{4},$$

Where V_b is the bulk volume of the core, d is the diameter of the core, and L is the length of the core.

The mass of dry core is measured. Then the core is vacuum saturated with brine for 1 hour. The mass of brine saturated core is measured after that. Gravimetric (Archimedes) method is used for pore volume calculation

$$PV = \frac{m_{saturated\ core} - m_{dry\ core}}{\rho_b}$$

Where PV is the pore volume of the core, $m_{saturated\ core}$ is the mass of brine saturated core, $m_{drycore}$ is the mass of dry core, and ρ_b is density of the brine saturated inside the core.

Then porosity (ϕ) is directly calculated as

$$\emptyset = \frac{PV}{V_b} \times 100\%$$

5.4.3 Preparation of Core Samples

The core samples are dried and cleaned. Teflon tape is used to wrap the core. The core is then placed in a plastic sleeve to cover all the wrapped core and then shrunk by heating it until the sleeve is well tight to the core. The prepared core is then placed in a rubber sleeve inside the core holder.

5.4.4 Particle Injection

The base case experimental data are measured as reference for comparison. The core sample is saturated with brine and vaporized with CO2 to dryness to determine the effect of mineral precipitation only on injectivity. The experiment is then repeated by replacing the initial saturating brine with colloidal solution.

A 600 ml piston cell of colloidal fluid is prepared to saturate the core. Quizix pump is used to inject the fluid into the core. The rate of injection is set to 0.5 ml/min and the backpressure regulator is set to 7 bar to ensure the core is well saturated with the liquid. The core holder is given a confinement pressure of 30 bar to ensure there is no leakage and liquid bypass through the core holder. The injection is done until the liquid in piston cell is finished. The experiment is repeated with different sandstone core sample, different size of particle, and by varying the concentration of colloids.

5.4.5 Supercritical CO_2 Injection

After saturating the core, the set-up is changed to supercritical CO_2 injection mode. The oven is set to 60 ^oC and the confinement pressure is raised to 160 bar. A 2500 ml piston cell filled with distilled water to collect effluent gas is connected to the outlet of the core. The backpressure regulator is set to 80 bar to ensure the CO_2 in supercritical phase. Supercritical CO_2 then is flooded into the core to displace and vaporize all the producible brine inside the core. CO_2 injection is stopped when the injected gas replaces water inside the piston cell. The

gas injection rate is varied from 2 ml/min, 5 ml/min, and 10 ml/min to study the effect of CO_2 injection rate.

5.4.6 Liquid CO_2 Pressure Drop and Permeability Measurements

The core sample is taken out of the set-up and dried at 60 ^oC for about 12 hours. After drying, the core is prepared into experimental set-up 2 for permeability measurement. The set-up is set to room temperature. The core holder is given 160 bar confinement pressure and outlet is connected to a piston cell filled with water. The backpressure is set to 80 bar to ensure the liquid phase of CO_2. The measurement is done until stable value is reached.

5.5 Analytical Methods

The parameter recorded in the particle and supercritical CO_2 experiment is the pressure drop across the core sample. The pressure drop is plotted against the dimensionless cumulative injected fluid (CIF). The pore volume of the core sample is the basis to determine the dimensionless volume.

5.5.1 Data Processing and Calculation

The injection rate is set from the pump before the injection. The injection time and pressure drop is recorded with LabVIEW software. The CIF volume is the time recorded multiplied by the rate of injection. The dimensionless CIF is directly obtained by divided CIF with pore volume of the core sample.

$$Dimensionless\ CIF = \frac{t \times q}{PV}$$

Where t is the time recorded (min), q is the rate of injection (ml/min), and PV is the pore volume of the core sample (ml).

5.5.2 Data Uncertainties

The liquid CO_2 measurement requires a constant discrete data. During the experiment, the uncertainty of data is often encountered. The uncertainty in data mainly comes from the differential pressure transducer. The pressure gauge gives fluctuation when recording the data. To reduce the uncertainty, the data is processed using mean value from statistical mode.

6 Results and Discussion

The experiments builds on earlier work conducted to study the effect of mineral deposition on CO_2 injectivity (Sokama-Neuyam *et al.*, 2015). Since the core was initially saturated with only brine in these earlier experiments, it serves as a benchmark for comparing the current experimental results where the saturating brine contains varying concentrations and sizes of colloidal particles. This benchmark results will be presented in the first part of this section followed by the series of particle injection experiments with varied concentration, injection rate, and varying initial core permeability. Table 7 and Table 8 respectively show the properties of the core samples and some initial properties of the experiments.

	Berea				Kirby		
	Core 1	Core 2	Core 3	Average	Core 1	Core 2	Average
Wet mass (g)	520.55	524.1	520.05		532.07	528.41	
Dry mass (g)	472.75	476.22	472.36		484.94	480.74	
PV(cc)	44.832	44.907	44.729	44.823	44.204	44.710	44.457
Porosity	0.1966	0.1969	0.1962	0.197	0.1939	0.1961	0.195

Table 7. Properties of core sample

Sandstone Core sample	Size of particle (μm)	Particle concentration (% w/w)			Gas injection rate (ml/min)		
Kirby	0.08	0.5			5		
Berea	0.08	0.3	0.5	1	2	5	10
	0.14	0.5			5		

Table 8. Overview of experiment performed

The initial permeability of the sandstone cores were measured with liquid CO_2. This gives the initial experimental data. Berea sandstone has higher permeability than Kirby sandstone. Table 8 below shows the initial CO_2 permeability of the two core samples.

	Berea	Kirby
Permeability (mD)	1210	345

Table 9. Initial permeability of sandstone core sample

6.1 Effect of Particle Concentration

The colloidal solution with particle size 0.08 µm was prepared with varying concentration and used as initial saturating fluid. The Berea core was initially saturated with colloidal solution of specific concentration and supercritical CO_2 was injected at a rate of 5 ml/min into the saturated core. The pressure drop profile was monitored in real time. When all producible colloids were displaced by CO_2 to dryness, the injectivity after fines migration was measured with liquid CO_2 and compared to the base case.

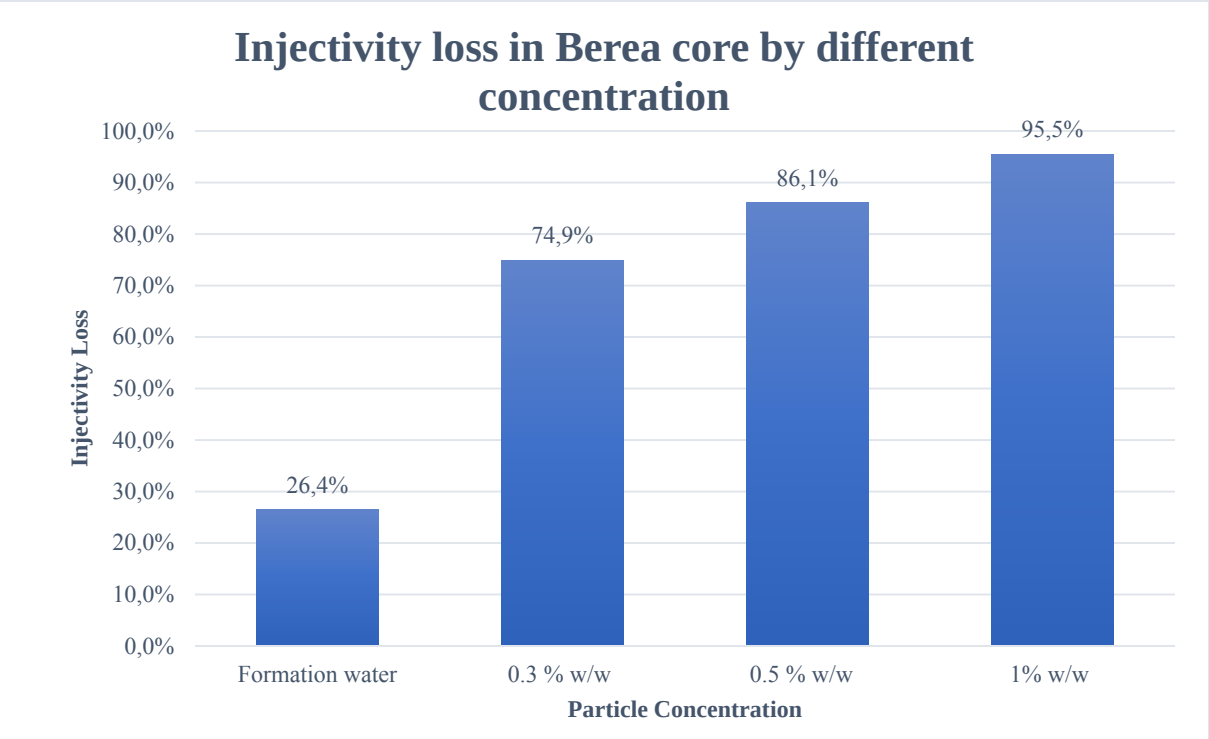

Figure 19. Effect of different particle concentration

Figure 19 shows that CO2 Injectivity loss increases with increasing particle concentration. The synthetic formation water gives the effect of mineral deposition in the reservoir and the particle colloidal solution shows the effect of mineral dissolution inside the reservoir. As particle concentration increases, the interaction between pore throat and particle also increases. This results in more retained particle and piping inside the pore throat. Since the pore throat constriction is further reduced, more energy is required to inject the same quantity of CO_2, leading to higher injectivity loss.

The saturation process could be used to explain the mechanism of particle trapping inside the pore throat. Higher concentration of particle gives more pressure drop across the core. In the

injection process, the effluent concentration and the initial concentration of colloids is observed to be the same in the experiment. No filter cake was seen after injection. Figure 20 shows the pressure drop when particle is injected into the core.

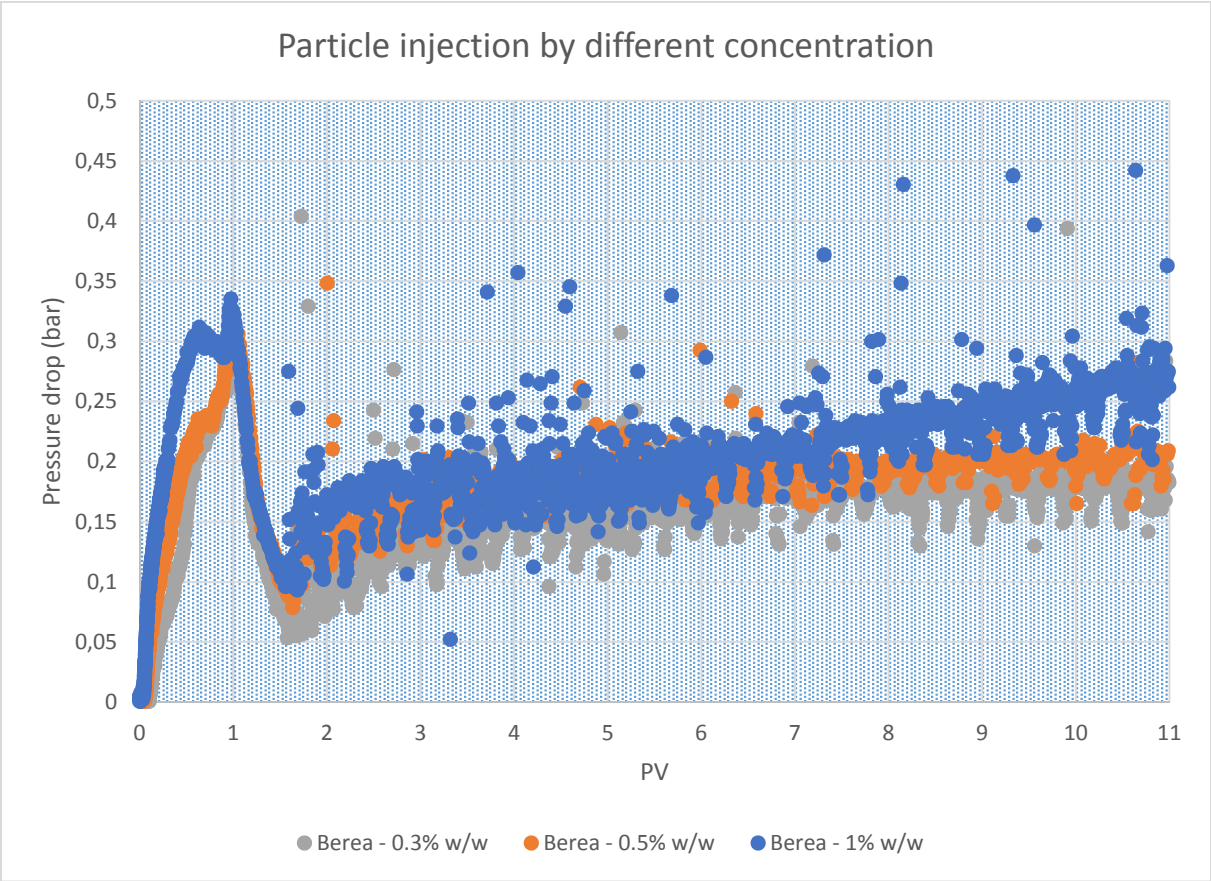

Figure 20. Effect of particle concentration in particle injection

In the beginning of the experiment, it was observed that the pressure drop built up to about 0.3 bar when the core was saturated with about 1 PV of colloidal solution (Figure 20). The fluid breakthrough after about 1 PV is injected into the core. A decline in the pressure drop is observed after breakthrough when the fluid reaches the outlet. Once the outlet pressure is stable and close to the backpressure, the pressure drop builds up again to steady condition.

Higher concentration of particle is expected to impose higher pressure drop. The chance of particles plucking the pore channels increases with increasing number of particles per volume of fluid injected. As the concentration of particles increases, more particles are available within the fluids at any time during the injection to bridge or pluck the pore throats. As more pores are bridged, the passage of flow is reduced and more energy is expended to push the same amount

of fluid through the core. Therefore, the rock permeability decreases and the pressure drop increases significantly.

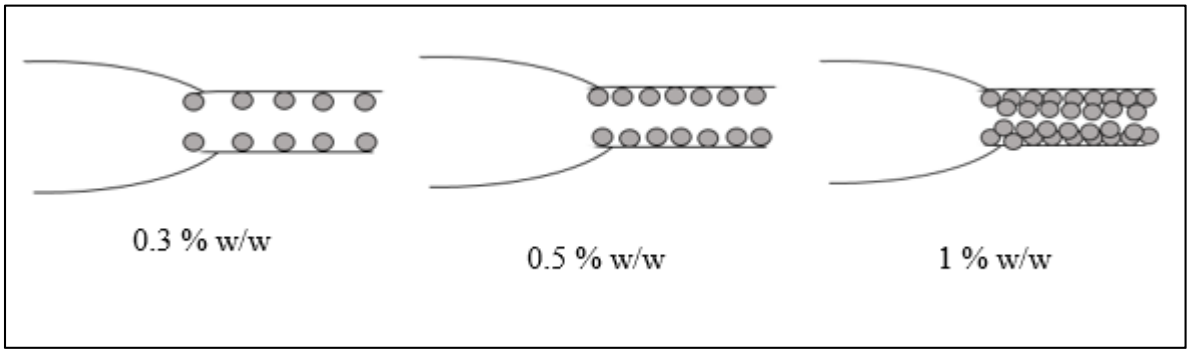

Figure 21. Graphical sketch of particle deposition in each concentration

Figure 21 shows the schematics of how particle deposited plug the pore throat. We observe from the sketch, deposition of lower concentration particle left more space for fluid to travel through the pore throat but deposition of higher concentration particle left less space. The size of pore throat is significantly decreased in higher particle concentration. Some of the particles also create multiparticle bridging in the pore throat. This resulted in blockage and completely plugging in pore throat.

Perhaps the most significant observation is that even small amount of particles induced high injectivity loss. As low as about 1% W/W of particles could pluck the pores and reduce injectivity to the barest minimum because most of the pore bridging occurs around the inlet region where the fluxes are highest. This emphasises that mineral dissolution and fines migration could have greater impact on Injectivity compared to salt precipitation.

Supercritical CO_2 injection pressure drop profile in Figure 22 & 23 confirm the effect of particle concentration on injectivity loss. More pressure drop is required to inject 5 ml/min supercritical CO_2 when the concentration of particle is increased. The pressure drop of each concentration shows similar profile with different magnitude of pressure drop.

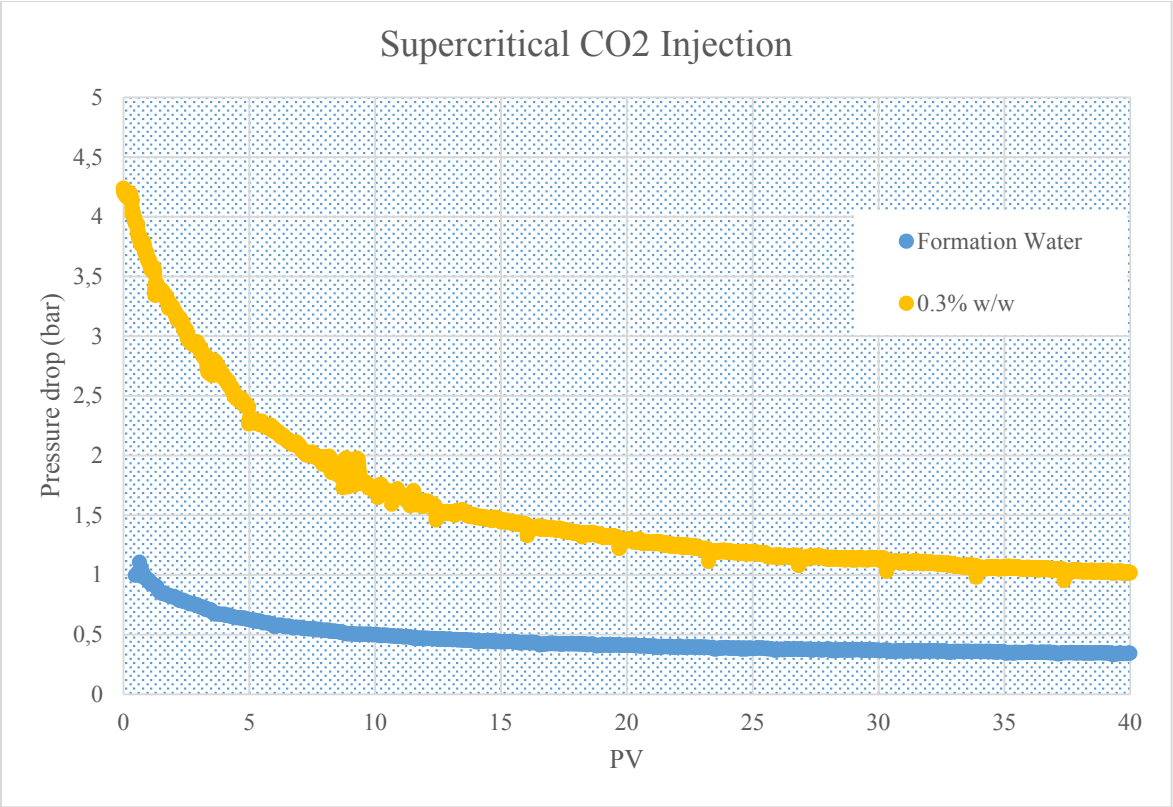

Figure 22. Pressure drop profile of supercritical CO2 injection with formation water and 0.3% w/w particle

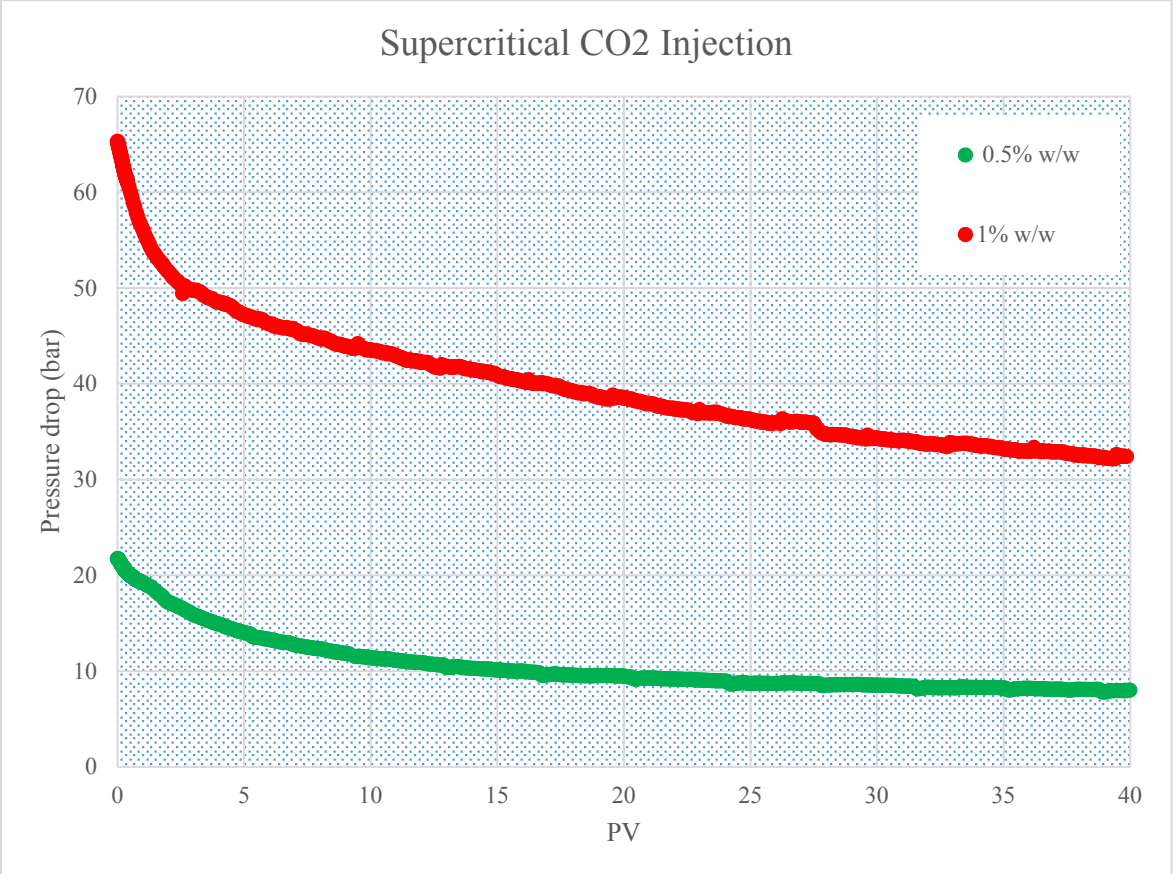

Figure 23. Pressure drop profile of supercritical CO2 injection with 0.5% w/w and 1% w/w particle

The interaction of CO2 and formation water in CCS operation could dissolve and precipitate minerals in the reservoir. Particles could detach from the pore walls to feed fines migration inside the pore throat. The fine particles could be transported by the injected fluid into the pore channels to impair permeability and restrict fluid flow. This experiment shows that mineral dissolution could impose significant effect on injectivity loss. As more minerals are dissolved and detached from the rock, injectivity of reservoir could decline even further.

6.2 Effect of Particle Size

Two Berea sandstone cores were initially saturated with colloidal solution containing particles of sizes, 0.08 µm and 0.14 µm and concentration of 0.5 % w/w. The result of injectivity loss is presented in Figure 24.

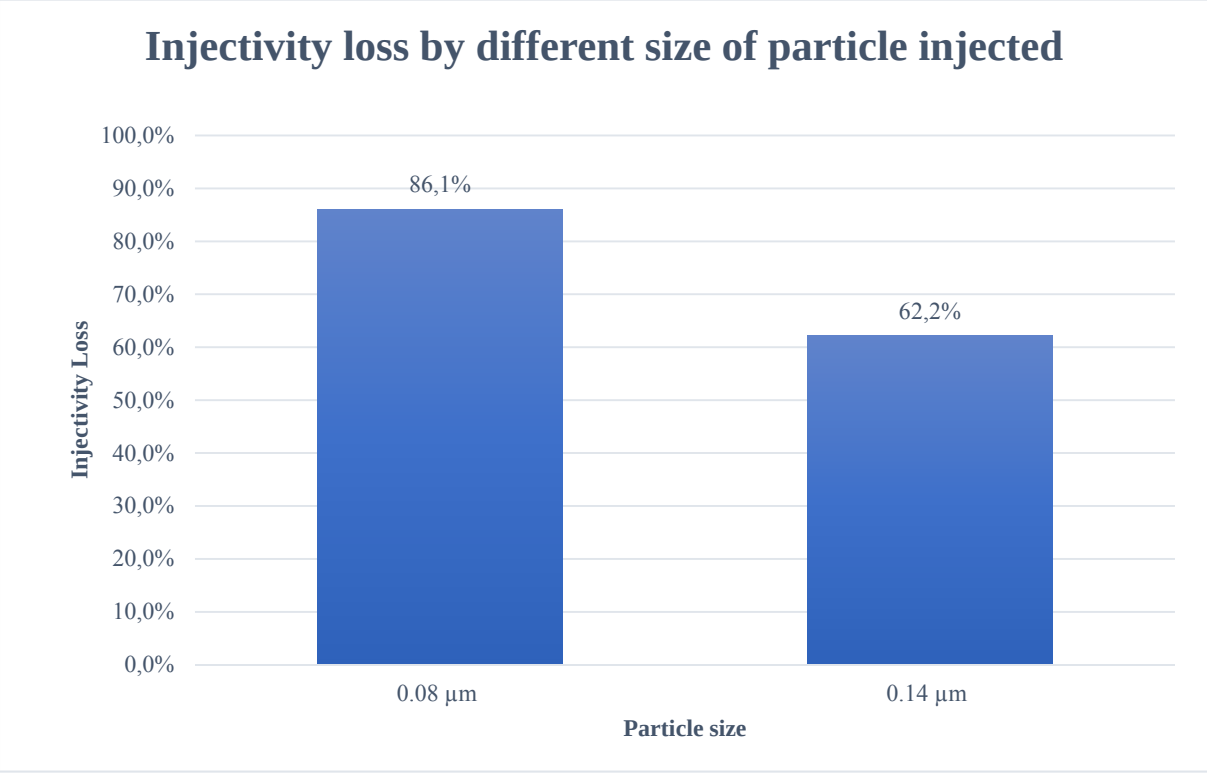

Figure 24. Effect of different particle size

The experimental results shows that bigger particles imposed lower injectivity loss in the core. Theoritically, this is contrary to observations reported by Khilar & Fogler (1998). They reported that plugging or piping occurence in pore thorat depends on the ratio of the size of fines to the size of pore throat. The higher the ratio, the more plugging and piping occurance inside the pore throat. The inconsistency of the current result is because the larger particles aggregates around

the inlet to form a filter cake. When the size of particle is equal or larger than the size of pore throat, there will be layer of particles or filter cake built up in front of the core which prevents the incoming particles from entering the core.

From the experiement, the effluent concentration and initial concentration of particle was the same. A filter cake was seen around the core sample after injection with 0.14 µm particle. The picture of filter cake is shown in Figure 25.

Figure 25. Filter cake in Berea sandstone core after injected with 0.14 µm particle

Filter cake is formed in the core inlet is an indication of plugging and size exclusion because of the particles. The distribution of the injection pressure from the centre to the outer side of core inlet adds more effect to the formation of filter cake. It leaves less energy to be applied to the particle at the outer side of the core inlet. The pressure drop of injection profile is shown in Figure 25.

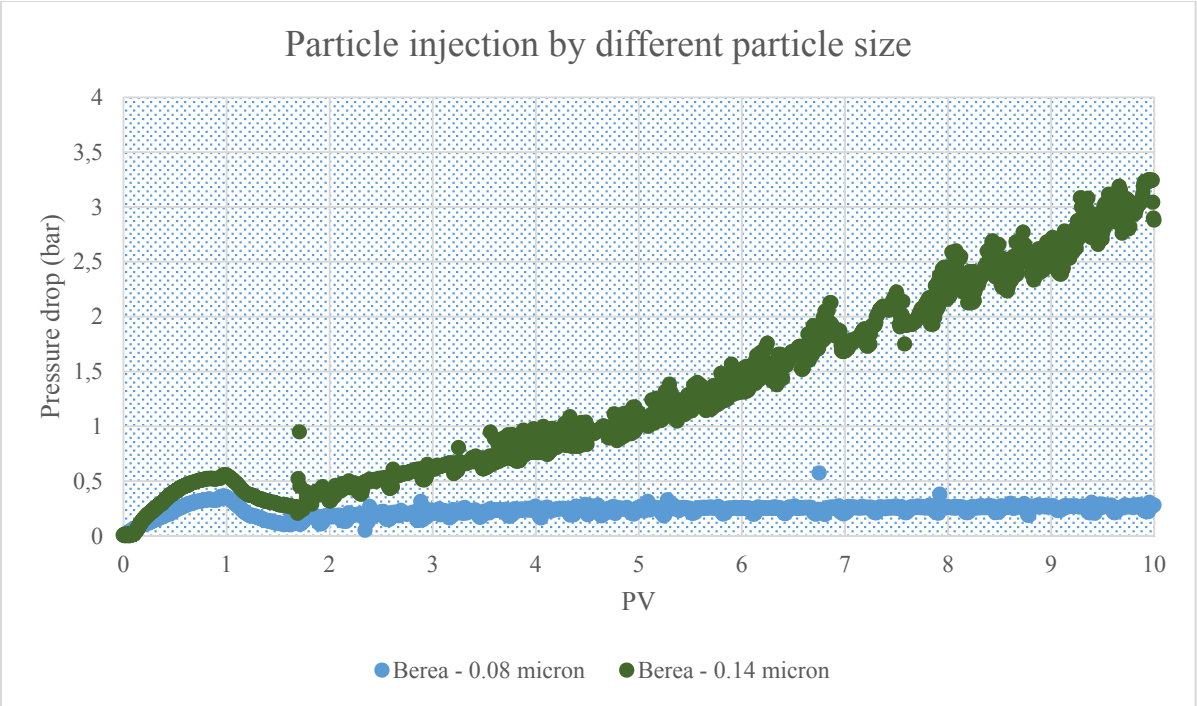

Figure 26. Effect of particle size in particle injection

A scatter point in the pressure drop is indication of the particle movement inside the pore throat. Khilar & Fogler (1998) reported that the ratio of the particle to the pore throat is a crucial parameter to determine if piping or particle entrapment will occur during particle injection. The particles with size of 0.08 µm give a steady and flat pressure drop profile (Figure 25). This indicates that particles are piping inside the pore throat. It reduces the pore throat size but it can still allow the particles to move within the pore channels.

Meanwhile, the particles with size of 0.14 µm shows a higher pressure drop in the beginning and increasing pressure drop when more particle is injected. Perhaps particles were trapped during the injection especially around the inlet. Initially, the larger particles forms a filter cake around the inlet that plug the cores and diverts the incoming particles to find neighbouring pores that have not been plugged. The accumulation of particles at the inlet raises the pressure drop as observed in the Figure 26.

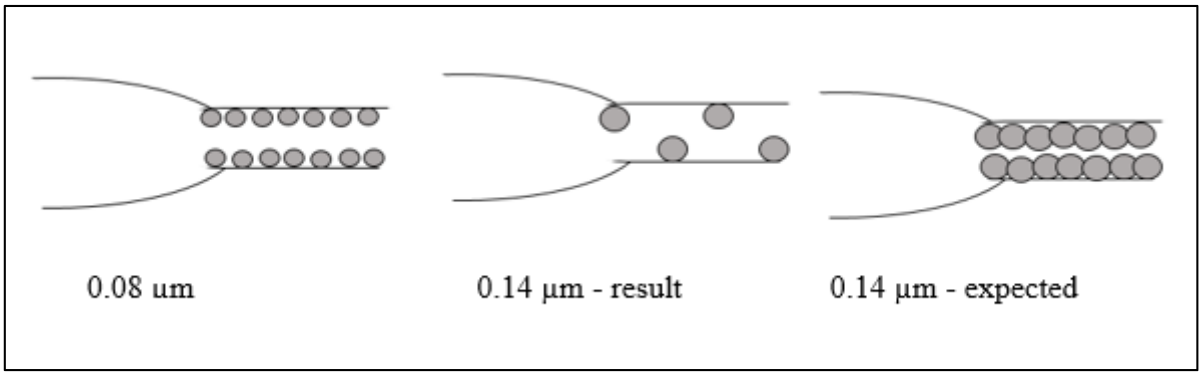

Figure 27. Graphical sketch of particle deposition in different particle size

From Figure 27 we can see the particle deposition accumulated in the pore throat. Particles create less space for pore throat inside the core. In the experiment, filter cake in larger particle restricted more particles to come into the pores. It imposes less particles come into the core and fewer pore throats is plugged. However, there is no outside filter cake formation in the reservoir resulted more blockage in the pore throat by larger particle.

The vaporization process from supercritical CO_2 in Figure 28 shows relevant result of injectivity loss. The bigger size of particle produced a lower pressure drop profile. This is because it leaves more unplugged pore throat inside the core which facilitates flow of CO_2 through the pore throats. The pressure drop profile of supercritical CO_2 injection shows a representative result.

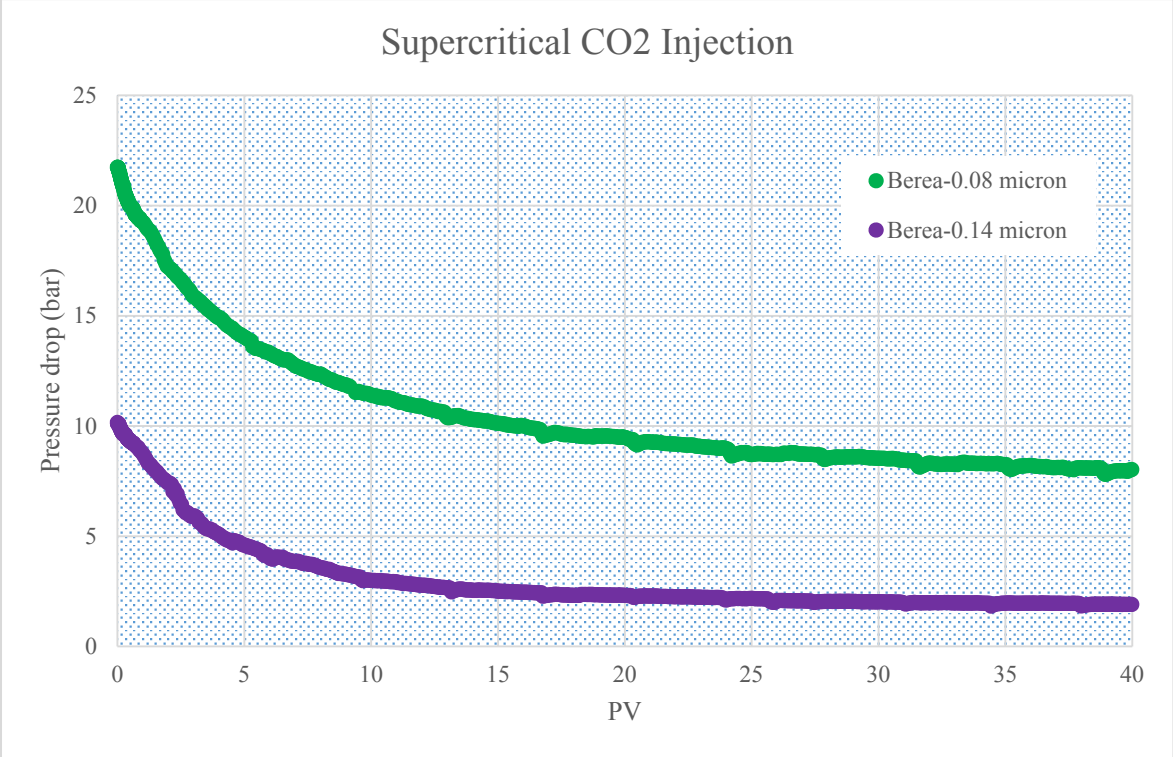

Figure 28. Pressure drop profile of supercritical CO2 injection with 0.08 µm and 0.14 µm particle

The experiment does not represents the practical mechanism of larger particle migration inside the reservoir. Practically, mineral dissolution and migration occurs within the reservoir. Therefore, outside filter cake cannot affect this process. The particle with bigger size will detach and travel inside the pore throat. This will result to even higher injectivity loss in the reservoir.

6.3 Effect of Rock Permeability

Colloidal solution that contains particles with concentration of 0.5 % w/w and size of 0.08 µm was injected into Berea and Kirby sandstone. The experimental result in Figure 29 shows that Berea core had more injectivity loss compared to Kirby core. The low permeability of Kirby sandstone means it has narrower pore throats. The narrower pore throat in Kirby sandstone give restriction to the particle as it moves within the pore throat. A filter cake is formed in front of the core inlet because of size exclusion.

It was observed that the filter cake covered all the surface of core inlet. Figure 30 shows a white layer of filter cake from the centre to the outer side of core inlet. Most of the particles were trapped at the outside before coming into the pore throat during injection. Fewer particles plugged the pore throat inside the core causing lower injectivity loss.

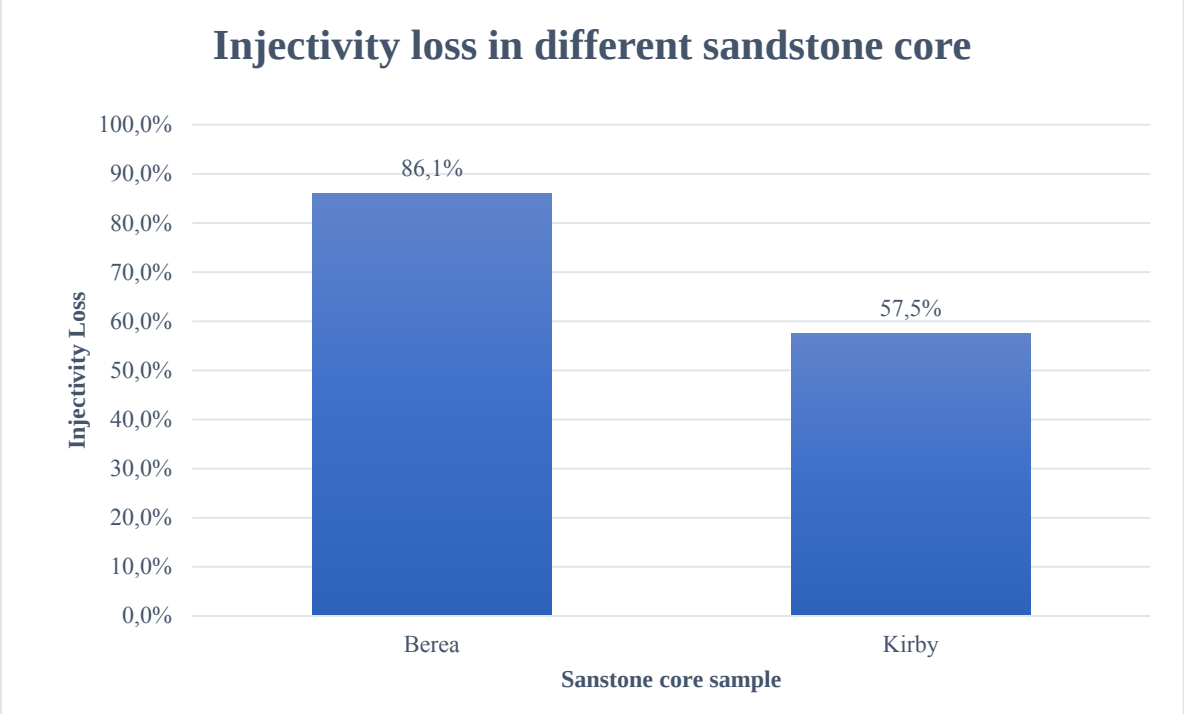

Figure 29. Effect of different rock permeability

Figure 30. Filter cake in Kirby sandstone core

The pressure drop profile of injection performance from different sandstone core give significant evident. From figure 31, the pressure drop in Kirby sandstone is higher than Berea sandstone. The difference in permeability between two sandstone core samples gives insight of the pore size distribution and interconnectivity.

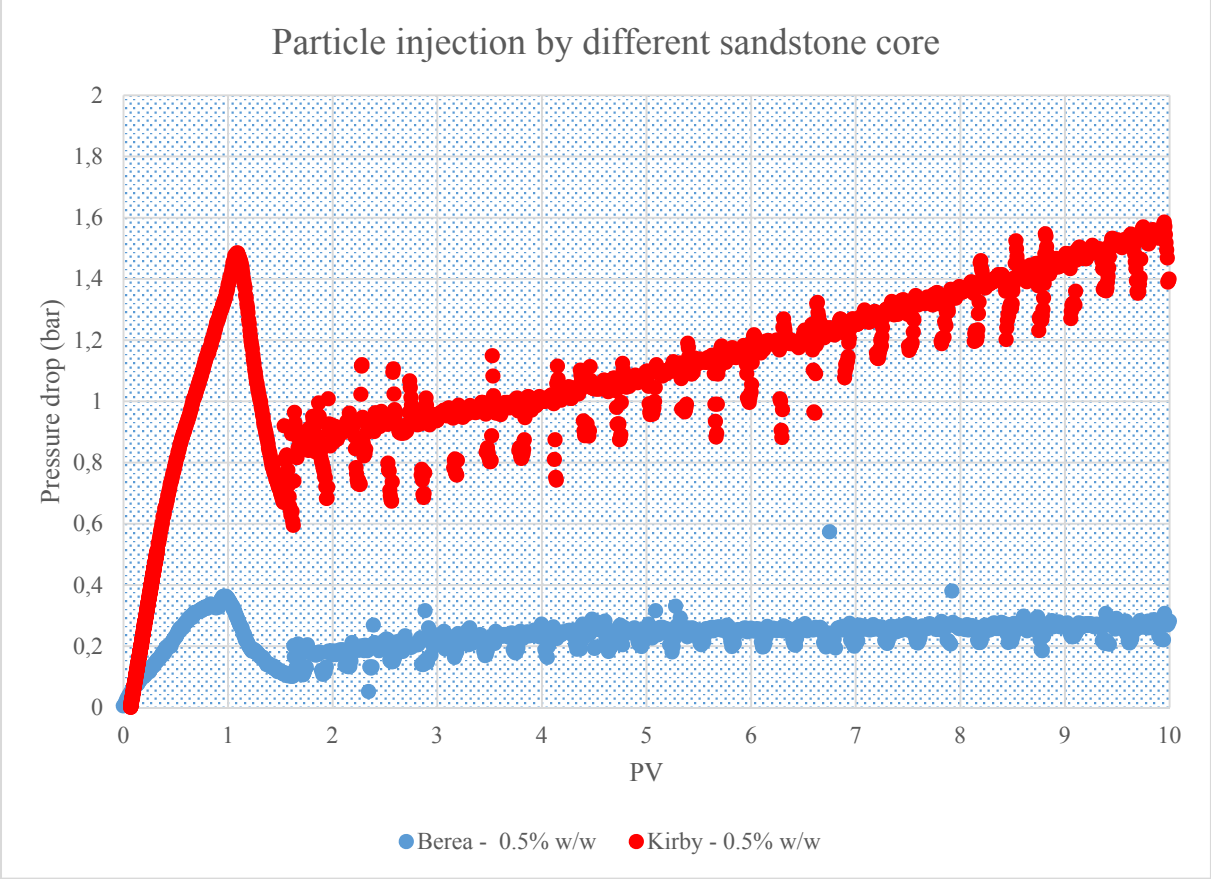

Figure 31. Effect rock permeability in particle injection

Kirby sandstone has lower permeability than Berea sandstone, it suggests that Kirby has smaller pore size distribution and poorer pore interconnection than Berea Sandstone. Therefore, the chances of particle entrapment inside the pore throat is higher for the core with smaller pore size distribution. Therefore, plugging is most likely to occur in low permeability rock. As more particles are injected into the core, the pressure drop increases. This indicates that the particles are accumulating inside the pore throat. In the Kirby sandstone, the particles accumulates in front of the core through size exclusion.

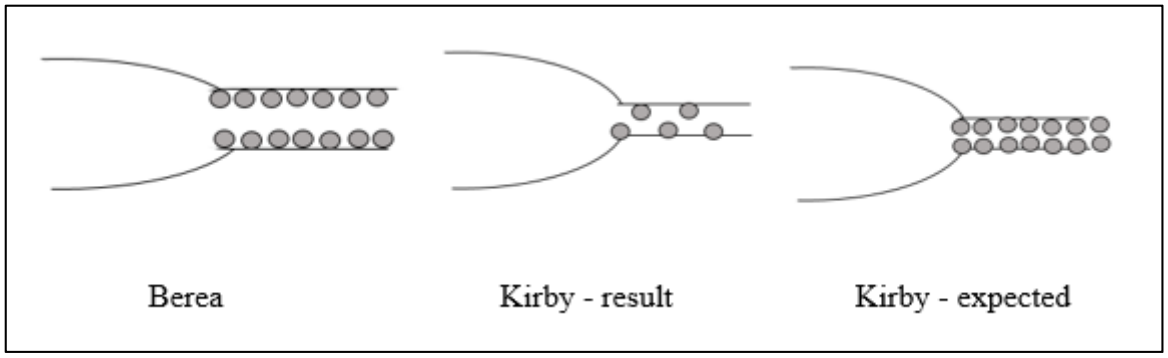

Figure 32. Graphical sketch of mineral deposition in different core

Figure 32 shows the schematic of mineral deposition in high and low permeability core. The particle deposited in high permeability core, Berea, has larger space in pore throat which can allow the fluid to transport. But Kirby, low permeability core, has smaller space left in pore throat. In reservoir, it would reduce significantly the size of pore throat. The ratio of size of fines particle to size of pore constriction is close to 1. Plugging and blocking mechanism would most likely occur and resulted more injectivity decreased. However, filter cake formation in experiment resulting less particles come into the core. Less particles deposited in the pore throat leaves more space to transport the fluid. It also causes less particles block and plug the pore throat.

The pressure drop profile from supercritical CO_2 injection shows the effect of particle plugging inside the core. Kirby sandstone has less particle coming into the pore throat compared to Berea sandstone. The amount of pressure drop in Berea Sandstone is higher than the amount of the pressure drop in Kirby sandstone (Figure 33).

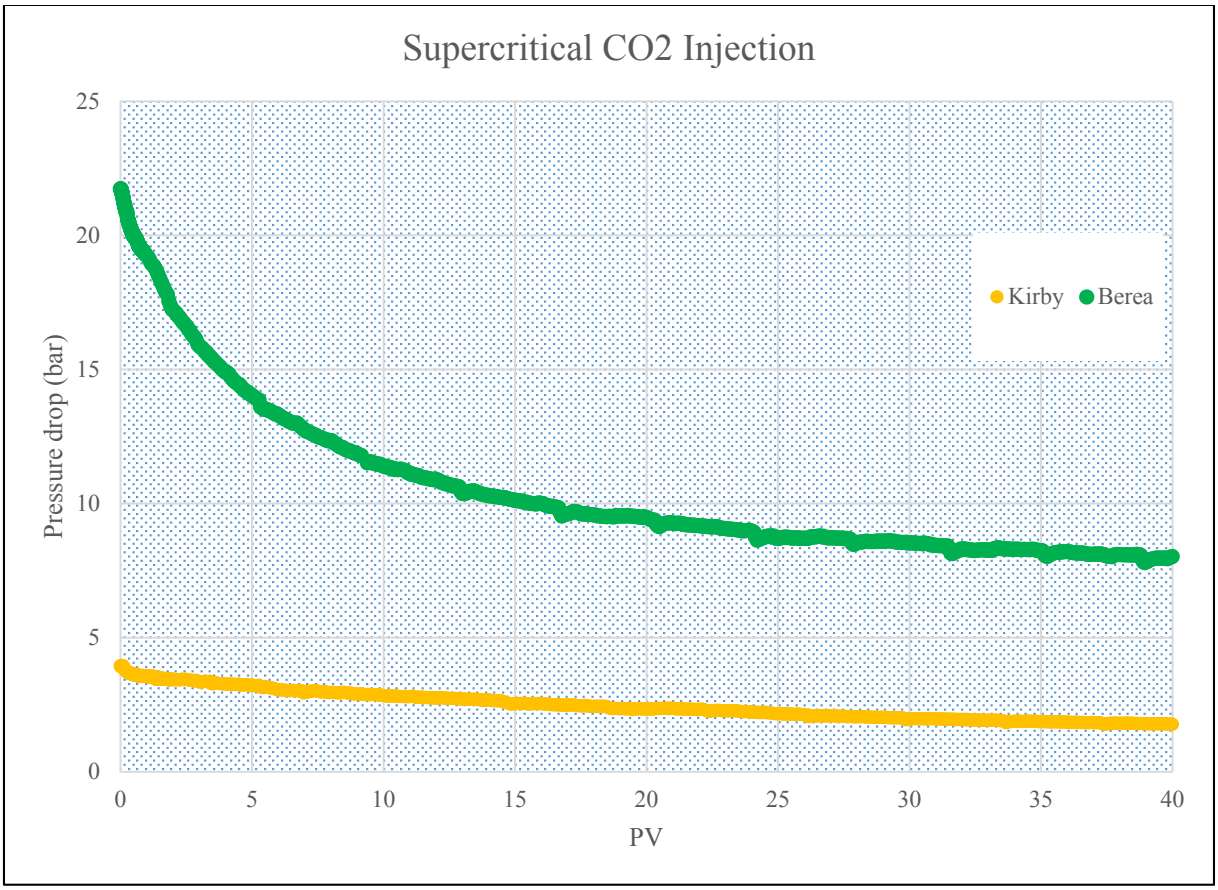

Figure 33. Pressure drop profile of supercritical CO2 injection with Berea and Kirby sandstone

The mineral dissolution process occurs within the pores. The lower permeability reservoir will provide higher ratio of the size of particle to the size of pore throat. The filter cake will not formed at the inlet, instead there will be particle blocking that will cause a severe injectivity loss. If all the particle injected could be transported into the Kirby sandstone core, and no filter cake was formed, the injectivity loss is expected to be higher than in Berea sandstone. Therefore, in the real reservoir, higher injectivity loss will be expected in the lower permeability rock because the pore throat is more easily plugged by the mineral.

6.4 Effect of Gas Injection Rate

The Berea sandstone core was initially saturated with 0.5 % w/w colloidal solution. The rate of supercritical CO_2 injection was varied from 2 ml/min, 5 ml/min, and 10 ml/min. CO_2 injectivity loss then was measured with liquid CO_2 at flow rate of 5 ml/min. The result of the experiment is presented in Figure 34. It was observed that Injectivity loss increases with increasing rate of supercritical CO_2 injection.

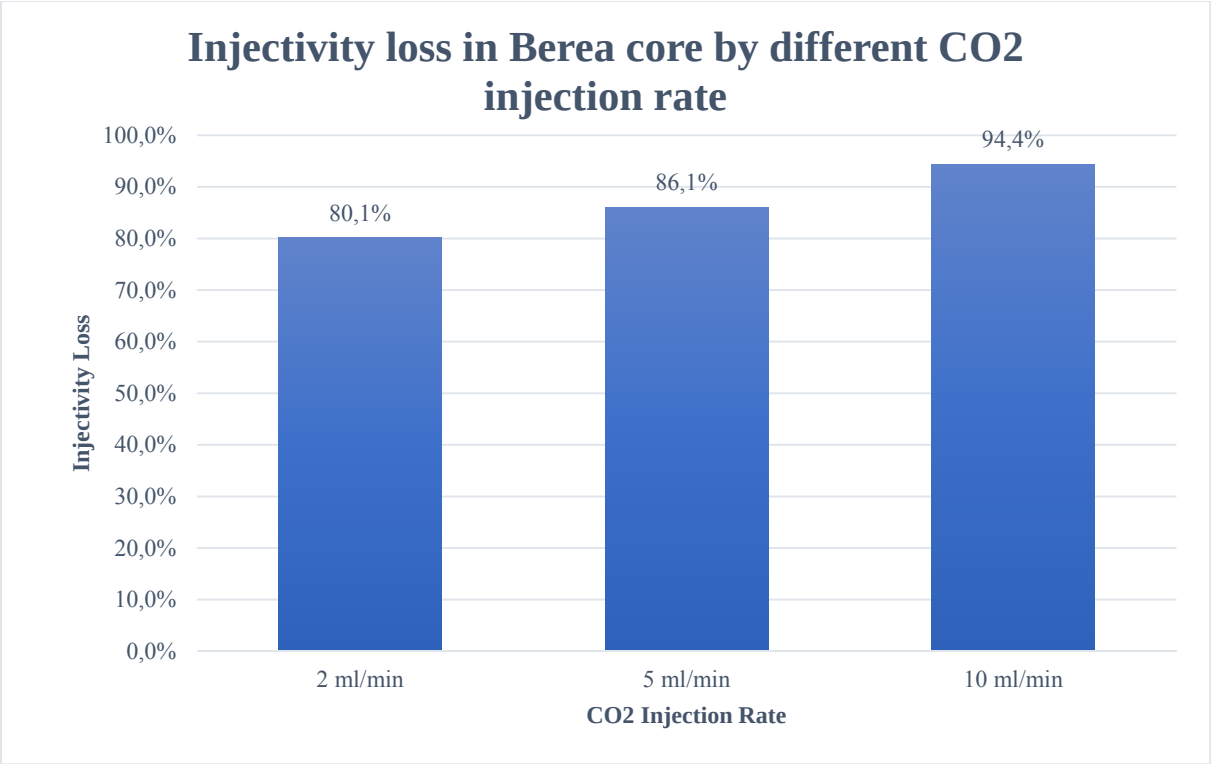

Figure 34. Effect of different gas injection rate

In the saturation process, the particles filled up the pore space and plugged the pore throat. Because saturation process only use low injection rate and injection pressure, particle only find and fill the empty porous spaces. During supercritical CO_2 injection, the injection pressure is set higher to obtain supercritical CO_2 phase. Turbulence from high injection rate gives more force to the particles resulting in redistribution of the particle inside the pore throat. The higher rate of randomization that emanate from higher CO_2 flow increases pore plugging. This could explain why injectivity is increased when the gas injection rate is increased.

In 5 ml/min of gas injection rate, supercritical CO_2 injection profile in Figure 35 shows why the injectivity loss is increased when the gas injection rate is increased. Initially, the injected CO_2 displaces the resident colloidal solution. This process is followed by capillary back flow. This is the combination of displacement and evaporation of unmovable brine inside the core. Brine is moving back and having more exposure to CO_2. The supercritical CO_2 gradually evaporates the unmovable brine and redistribute particle inside the pore throat.

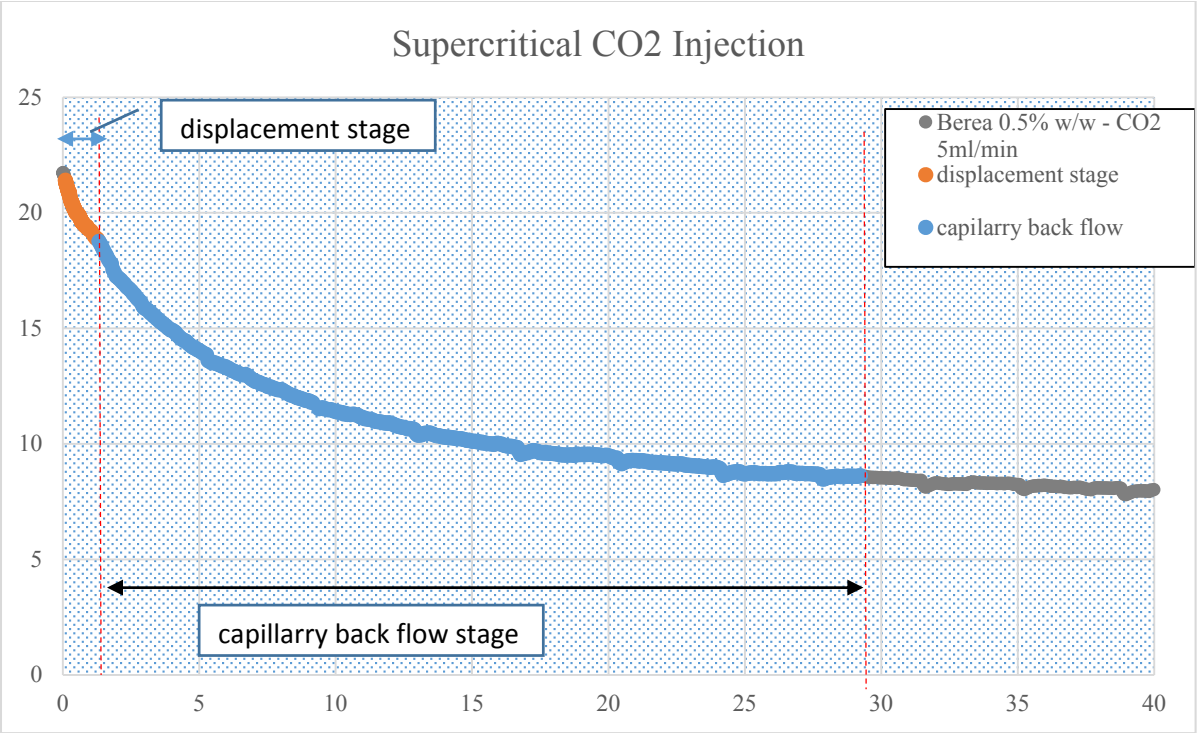

Figure 35. Supercritical CO2 pressure drop profile

The pressure drop profile is analysed with semi log plot. From Figure 36, the gradient of trend line is changed after one process is finished. Displacement stage is followed by capillary back flow with steeper gradient. The pressure drop profile is expected to be flat in the end phase if more supercritical CO_2 was injected into the saturated core. However, the evaporation process is not visible because of limited volume of CO_2 injected.

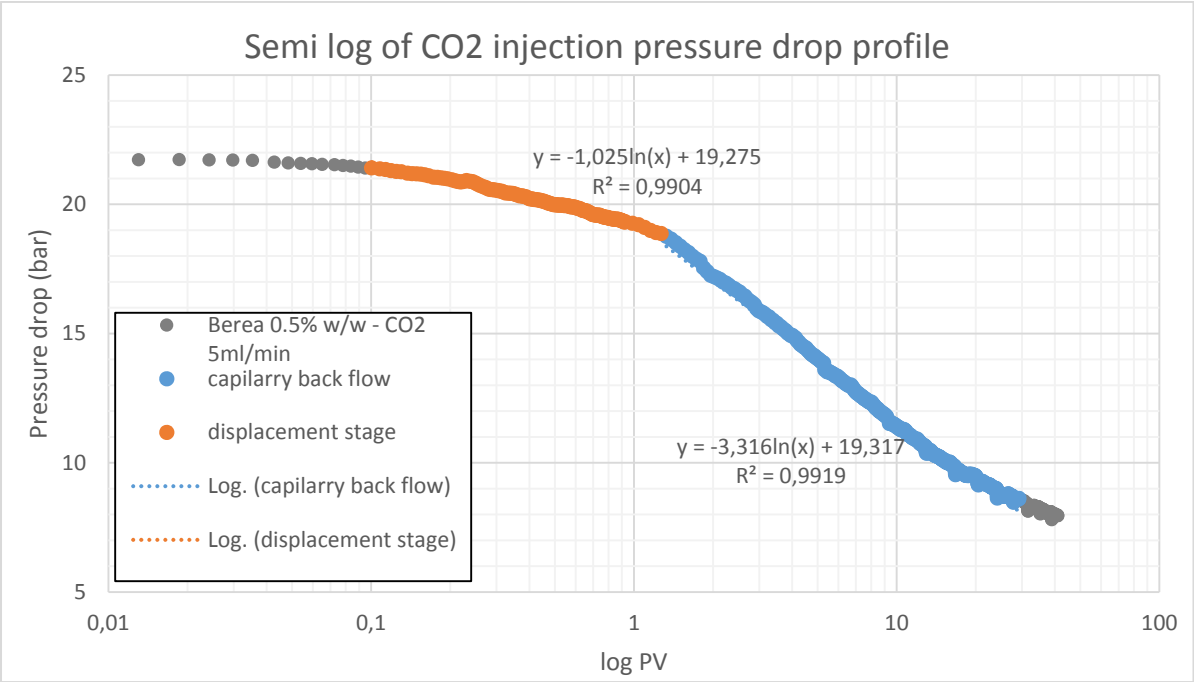

Figure 36. Semilog plot of CO2 injection pressure drop profile

The pressure drop profile shows the flow restriction when the gas is injected into particle saturated core. From the Figure 37, there is high flow restriction when the gas is injected with higher flow rate. The end of pressure drop lays in the order from up to bottom according to the injection rate.

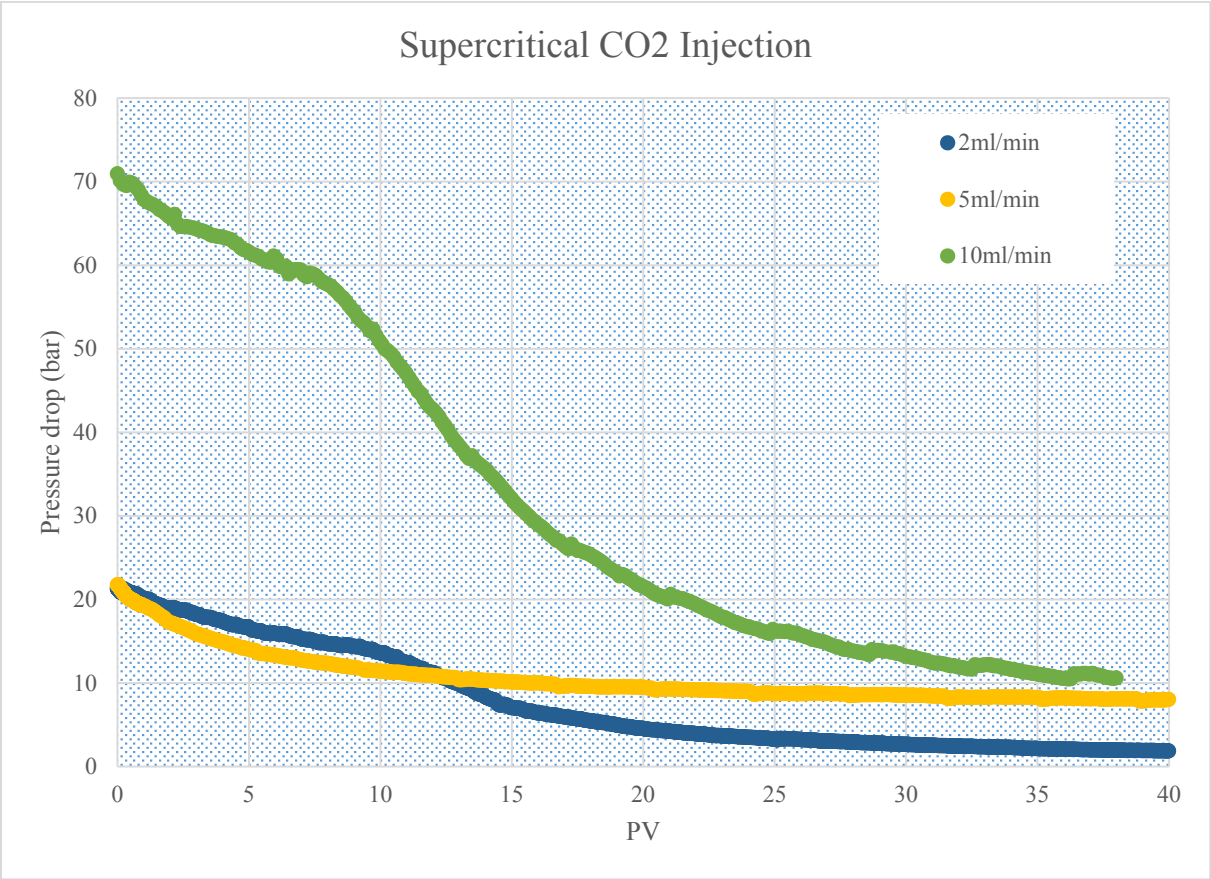

Figure 37. Pressure drop profile of supercritical CO2 at differerent injection rate

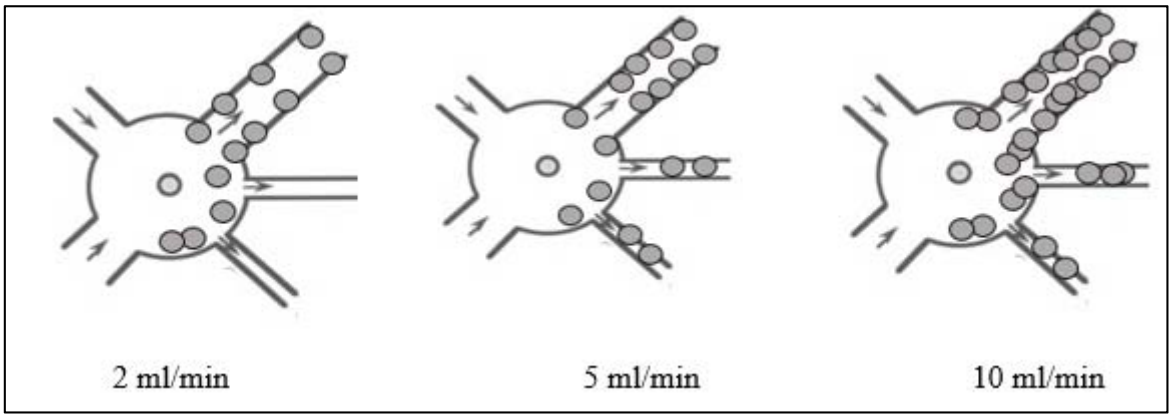

Figure 38. Graphical sketch of particle plugging mechanism with varied CO2 injection rate

The pressure drop profile (Figure 37) at rate of 10 ml/min and 2 ml/min look similar in shape. Initially, the supercritical CO_2 injection pressure drop is similar in shape for all three pressure

profiles. At 10 ml/min and 2 ml/min, the pressure profile suggests that different mechanism is at play. The particle-pore interactions seems to change for varying rates. Figure 38 shows the possible mechanism of particle plugging inside the pore network. The force from injection is pushing more particles into the pore throat. The turbulence from different rate is redistributing the particle to all pore network. Lower injection rate decrease the probability to plug the smaller pore throat because it has less energy to push and distribute particle. Higher injection rate stack more particles into the pore throat and even push more particle to smaller and plugged pore throat. It resulted less space in pore network to transport the gas. This could be the possible reason for different pressure drop profile in supercritical CO_2 injection process.

Different CO_2 injection rate in CCS operation can impose different effect on CO_2 injectivity. High injection rate can lead to injectivity loss and economic challenges. Proper planning and scenario of the storage operation needs to be investigated.

7 Conclusion

The experiments have been successfully conducted to investigate the effect of colloidal transport on CO_2 injectivity. The results obtained from experiment are summarised as follows:

- Particle concentration gives significant effect on CO_2 injectivity. Moderate amount of fines migration in the reservoir could plug the pore throat of the reservoir and decrease injectivity significantly.
- Injectivity loss is lower when the core is initially saturated with larger particle solutions. A filter cake is found in front of the core due to size exclusion and filtration. However, a bigger particle size in fines migration will plug more pore throat and result in higher injectivity loss.
- The low permeability core showed lower injectivity loss. Thin layer of filter cake is also seen in front of the core. The filtration effect from the filter cake resulted in less amount of particle plugging in the pore throat. But fines migration in low permeability reservoir does not form filter cake.
- The injectivity loss increased with increasing CO2 injection rate. The turbulence from the higher flow rate make the particle stack tighter and redistributed evenly in the pore network.

This experimental work is useful to recreate the mineral dissolution process and fines migration during CO_2 storage operation in sandstone formations. It gives information about the process and qualitative effect on injectivity loss for further planning and operation scenario of CO_2 injection.

Future Work

This research give good understanding of CO_2 injectivity in the fines migration process. However, the research can be extended study about CO_2 injectivity change, mechanism and effect. Some recommendations for further research are:

- The same experiment in supercritical CO_2 injection can be performed to investigate the displacement, back flow, and dry out process inside the core. This research can be used to predict time and volume allocation of CO_2 injected with optimum injectivity.

- A research with oil saturated core to investigate the recovery of oil with CO_2 injection under fines migration process. This proposal also predict displacement stage process and volume of CO_2 injected.
- A study of mathematical model from experimental result to estimate how much injectivity loss with certain concentration of particle and salt in colloidal solution.

8 References

Alden, A. (2013). *http://geology.about.com/od/more_sedrocks/a/about sandstone.htm*.

Bacci, G., Korre, A., & Durucan, S. (2011). Experimental investigation into salt precipitation during CO_2 Injection in saline aquifers. *Elsevier*.

Bachu, S. (2003). Screening and ranking sedimentary basins for sequestration of CO_2 in geological media in response to climate change. *Environmental Geology*, 277-289.

Basu, S., & Sharma, M. (1997). Effeect of Floodwater Salinity on Recovery of Oil From Cores Containing Clays. *Annual California Regional Meeting of SPE of AIME.* Los Angeles.

Biglarbigi, K., Mohan, H., & Carolus, M. (2011). The Costs and Benefits of Carbon Capture Storage. *Offshore Technology Conference.* Houston.

Buret, S., Nabzar, L., & Jada, A. (2010). Water Quality and Well Injectivity: Do Residual Oil-in-water Emulsion Matter? *SPE JOurnal*, 557-568.

Carlson, G. (2000). Experimental Errors and Uncertainty . 1-6.

Cerasi, P., Kjoller, C., & Sigalas, L. (2016). Mechanical effect of CO_2 Flooding of a sandsotne specimen. *Energy Procedia*, 361-370.

Churcher, P., French, P., Shaw, J., & Schramm, L. (1991). Rock Properties of Berea Sandstone, Baker Dolomite, and Indiana Limestone. *SPE International Symposium on Oilfield Chemistry.* Anaheim.

Dawson, G., Pearce, J., Biddle, D., & Golding, S. (2014). Experimental mineral dissolution in Berea Sandstone reacted with CO_2 or SO_2-CO_2 in NaCl brine under CO_2 sequestration conditions. *Elsevier*.

Deer, W. (1992). An introduction to the rock-forming minerals. *Longman Scientific & Technical*.

Enick, R., & S.M., K. (1990). CO_2 Solubility in water and brine under reservoir conditions. *Chem. Eng. Comm.*, 23-33.

Fallah, H., AHmadi, A., Karae, M. A., & Rabani, H. (2012). External Cake Build Up at Surface of Porous Medium. *Journal of Fluid Dynamics*.

Fjelde, O., Polanska, A., Tagjiyev F.T., & Asen , S. (2013). Low Salinity Water Flooding: Retention of Polar Oil Components in Sandstone Reservoir. *IOR 2013 - 17th European Symposium on Improved Oil Recovery.* St. Petersburg.

Galal , S. K., Elgibaly, A., & Elsayed, S. K. (2105). Formation damage due to fines migration and its remedial methods. *Elsevier*.

Gale, J., & Freund, P. (2001). Coal-bed methane enhancement with CO_2 sequestration worldwide potential. *Environmental Geosciences*, 210-217.

Grigg, R. (2005). Long-term CO_2 Storage : Using Petroleum Industry experience, Carbon Dioxide Capture for Storage in Deep Geologic Formations- Result from the CO_2 Capture Project, v. 2: Geologic Storage of Carbon Dioxide with Monitoring and Verification. *Elsevier*, 853-866.

Guedes, R., Al-Abduwani, F., Bedrikovetskty, P., & Currie, P. (2006). Injectivity Decline Under Multiple Capture Mechanisms. *SPE International Symposium and Exhibition on Formation Damage Control.* Lafayette.

(2011). Huhne Opens UK's first CCS plant. (Huhne, Interviewer)

IEA. (2016). *Prospects for CO_2 Capture and Storage.*

Institute, A. P. (1968). *API recommended practice for analysis of oil-field waters.* American Petorleum Institute.

IPCC. (2005). *Carbon Dioxide Capture and Storage.* Cambridge: Cambridge Unversity Press.

Jadhunandan, P., & Morrow, N. (1995). Effect of Wettability on Waterflood Recovery for crude -Oil/Brine/Rock Systems. *SPE Reservoir Engineering*, (pp. 40-46).

Kaarstad, M. O. (2008). Experience from real CCS Projects - and the way forward. *World Petroleum Congress.* Spain.

Khilar, K. C., & Fogler, H. S. (1998). *Theory and Applications of Transport in Porous Media Migration of Fines in Porous Media.* Springer.

Kohl, A., & R.B, N. (1997). *Gas Purification.* Houston: Gulf Publishing Company.

Kubus, P. (2010). CCS and CO_2-Storage Possibility in Hungary. *SPE International Conference on CO2 Capture, Storage, and Utilization.* New Orleans.

Lacis, A., Schmidt, G., Rind, D., & Ruedy, R. (2010). Atmospheric CO_2 : Principal Control Knob Governing Earth's Temperature. *Science*, 356-359.

Larsen, J. (2003). The effects of dissolved CO_2 on coal structure and properties. *International Journal of Coal Geology*, 63-70.

Lucci, A., Demofonti, G., Tudori, P., & Spinelli, C. M. (2011). CCTS (Carbon Capture Transportation & Storage) transportaion issues. *International Offshore and Polar Engineering Conference.* Maui.

Mubiayi, M. P. (2013). Characterisation of Sandstones : Mineralogy and Physical Properties. *World Congress on Engineering.*

Nimtz, M., Klatt, M., Wiese, B., Kuhn, M., & Krautz, H. (2010). Modelling of the CO_2 process- and transport chain in CCS systems-Examination of transport and storage processes. *Geochemistry*, 185-192.

O&GJ. (2010). Oil and Gas Journal.

Onarheim, K., Mathisen, A., & Arasto, A. (2014). Barriers and opportunities for application of CCS in Nordic industry - A sectorial approach. *International Journal of Greenhouse Gas Control*.

Pudlo, D., Henkel, S., Ezman, F., Katja, H., Werner, L., Ganzer, L., . . . Gaupp, R. (2014). The relevance of mineral mobilization and dissolution on the reservoir quality of sandstone in CO_2 storage sites. *Elsevier*.

Ramamurthi, K., & Sunil Kumar, S. (2003). Predicton of inception of thermal oscillations and thies waveforms in flow of heated subcritical liquids. *Heat and Mass Transfer*, 3359-366.

Sokama-Neuyam, Y. A., & Ursin, J. R. (2015). CO_2 Well Injectivity : Effect of Viscous Forces on Precipated Minerals. *IPTC.* Doha.

Sokama-Neuyam, Y. A., & Ursin, J. R. (2015). The Effect of Mineral Deposition on CO_2 Well Injectivity. *SPE*.

Span, R., & W., W. (1996). A new equation of state for carbon dioxide covering the fluid region from triple-point temperature to 1100K at pressures up to 800 Mpa. *Journal of Phys. Chem. Data*, 1509-1596.

Stangeland, A. (2007). Retrieved from www.bellona.org: http://bellona.org/news/ccs/2007-10-why-co2-capture-and-storage-ccs-is-an-important-strategy-to-reduce-global-co2-emissions

Statoil. (2010). *CCS - our history*. Retrieved from http://www.statoil.com/annualreport2009/en/sustainability/climate/pages/ccs-ourhistory.aspx

Sweatman, R., Crookshank, R., & Edman , S. (2011). Outlook and Technologies for Offshore CO2 EOR/CCS Projects. *Offshore Technology Conference.* Houston.

Wanga, Y., Mackieb, E., Rohana, J., Lucea, T., Knabea, R., & Appela, M. (2009). Experimental Study on Halite Precipitation During CO_2 Sequestration. *International Symposium of the society of core analysts.* Noordwijk.

Worden, R. H., & Morad, S. (2003). *Clay Mineral Cements in Sandstones.* Blackwell Science.

Zuluaga, E., & Monsalve, J. (2003). Water Vaporization in Gas Reservoirs. *SPE Eastern Regional Meeting.* Penssylvania.

9 Appendices

Table 10. Pressure drop and injectivity loss value by different type of solution

	Berea		Kirby	
	Pressure drop (bar)	Injectivity loss	Pressure drop (bar)	Injectivity loss
Initial	0.0735	0.0%	0.2575	0.0%
Formation water	0.0998	26.4%	0.6762	61.9%
0.3 % w/w	0.2921	74.9%		
0.5 % w/w	0.5276	86.1%	0.6055	57.5%
1% w/w	1.6176	95.5%		

Table 11. Pressure drop and injectivity loss value by different CO2 injection rate

	Berea		Kirby	
Rate	Pressure drop (bar)	Injectivity loss	Pressure drop (bar)	Injectivity loss
2 ml/min	0.3697	80.1%		
5 ml/min	0.5276	86.1%	0.6055	57.5%
10 ml/min	1.3021	94.4%	-	

Table 12. Pressure drop and injectivity loss value by different particle size.

	Berea	
Particle size	Pressure drop (bar)	Injectivity loss
0.08 μm	0.5276	86.1%
0.14 μm	0.1941	62.2%